

Systematics of High-Pressure Silicate Structures

L. W. Finger and R. M. Hazen

*Geophysical Laboratory
Carnegie Institution of Washington
5251 Broad Branch Road, NW
Washington, DC 20015*

INTRODUCTION

Mineral-like phases quenched from high-pressure synthesis experiments, as well as minerals formed in natural high-pressure environments, reveal crystal chemical principles that govern the formation of dense oxide and silicate structures. A systematic survey of known high-pressure silicate structures that incorporate octahedrally-coordinated silicon ($^{\text{VI}}\text{Si}$) is thus appropriate for this volume on the variation of crystal structures with temperature and pressure.

The pace of discovery of new high-pressure silicates is rapid. A decade ago, Finger and Hazen (1991) summarized the twelve known high-density structural topologies with $^{\text{VI}}\text{Si}$. By late 1999, twice that number had been described. Of the original dozen structure types, seven (stishovite, perovskite, ilmenite, hollandite, calcium ferrite, pyrochlore, and K_2NiF_4) contain only six-coordinated silicon. The five additional high-pressure silicates known at that time, including the garnet, pyroxene, wadeite, anhydrous phase B, and phase B structures, contain both $^{\text{IV}}\text{Si}$ and $^{\text{VI}}\text{Si}$.

Finger and Hazen (1991) used these twelve structure types to identify five systematic trends related to structural topology and isomorphous substitutions that might point to the existence of other high-pressure silicate structures. Two of these trends systematize groups of structurally related phases:

- (1) the structures of rutile, hollandite and calcium ferrite form from edge-sharing chains of silicon octahedra; and,
- (2) homologous structures in the system Mg-Si-O-H, including phase B and anhydrous phase B, feature edge-sharing clusters of twelve magnesium octahedra surrounding a silicon octahedron (Finger and Prewitt 1989).

The other three criteria recognize similarities between high-pressure silicates and room-pressure isomorphs. High-pressure silicates often have structure types that were first observed in:

- (3) room-pressure germanates with octahedrally-coordinated Ge, such as the germanium analog of phase B;
- (4) room-pressure oxides with octahedrally-coordinated 3+ or 4+ transition-metal cations, such as TiO_2 in the rutile structure, which is also observed in stishovite; or,
- (5) room-pressure aluminates, related to high-pressure silicates by the substitution $2(^{\text{VI}}\text{Al}) \Rightarrow ^{\text{VI}}(\text{Mg} + \text{Si})$, as observed in ilmenite, pyroxenes, and garnets.

In spite of the limited number of known $^{\text{VI}}\text{Si}$ structures, these five trends pointed to the probable existence of many more such phases. Indeed, the number of known high-pressure phases with $^{\text{VI}}\text{Si}$ has doubled since 1991, and new systematic structural trends have been identified. The principal objective of this chapter is to update Finger and Hazen (1991), by cataloging the known high-pressure $^{\text{VI}}\text{Si}$ phases. We identify and evaluate the systematic structural trends displayed by these phases, and predict additional structure types that might be produced at high pressure.

Mineralogical setting

Silicon and oxygen are the Earth's most abundant elements, and silicate minerals predominate throughout the Earth's crust and mantle (to a depth of about 2900 km). While hundreds of silicate structures have been catalogued (see e.g. Liebau 1985), only about 50 different structure types account for almost all of the volume of the crust and mantle (Smyth and Bish 1988). A common feature of low-pressure silicate structures is the presence of silicon cations exclusively in four coordination by oxide anions (^{IV}Si). Polymerization of SiO_4 groups dictates many mineral properties, and the topology of tetrahedral linkages provides the basis for most silicate classification schemes.

Research on silicates synthesized at high pressures and temperatures plays a major role in efforts to understand the Earth's deep interior. Crystalline materials erupted from depths of more than 100 km, extracted from shocked material associated with meteorite impacts, or produced in high-pressure laboratory apparatus provide a mineralogical glimpse into Earth's inaccessible deep interior. The first experiments on common rock-forming silicates at pressures up to 10 GPa revealed striking changes in mineral structure and properties. Sergei Stishov's seminal investigation of SiO_2 , for example, demonstrated the transition from a relatively open quartz framework of corner-sharing silicate tetrahedra to the dense rutile-type structure of stishovite, with edge-sharing chains of silicate octahedra (Stishov and Popova 1961, Hazen 1993, Stishov 1995). The corresponding increase in density—more than 66%, from 2.65 to 4.41 g/cm^3 between 0 and 8 GPa (Ross et al. 1990), has profound implications for the interpretation of seismic velocity data.

Subsequent high-pressure experiments have demonstrated that all common crustal silicates undergo phase transitions to new structures with ^{VI}Si between pressures of about 5 GPa (for some framework silicates) to about 20 GPa, which corresponds to the pressure at the top of the Earth's lower mantle. Many researchers now assert that the dominant mineral structure type in the Earth's lower mantle—indeed, the structure that may account for more than half of the solid Earth's volume—is perovskite of the approximate composition $(\text{Mg}_{0.88}\text{Fe}_{0.12})\text{SiO}_3$, in which silicon occurs in a corner-linked array of octahedra. Silicate perovskites, mixed with the oxide magnesiowastite $(\text{Mg,Fe})\text{O}$, may account for the relatively high seismic velocities of this region (670 to 2900 km) in which velocities increase relatively smoothly with depth. Mineral physicists identify silicon coordination number as the major crystal-chemical difference between the Earth's crust and lower mantle: Si is virtually all four-coordinated in lower-pressure phases, shallower than ~200 km, but is entirely six-coordinated in higher-pressure phases below 670 km.

The upper mantle and transition zone, which lie above the lower mantle, possess a much more complex seismic character with depth. This region, extending to a depth of 670 km, displays several discontinuities and changes in slope of the velocity-depth profile. Such features might be caused by either compositional variations or phase transitions. However, given the suspected pattern of mantle convection and the well documented variety of high-pressure phase transitions in silicates, the latter explanation seems the more plausible (Hazen and Finger 1978). Specific phase transitions have been proposed for each of the major seismic features and mineralogical models have been proposed that account for most of the complexities between 200 and 670 km.

SURVEY OF ^{VI}SI STRUCTURES

This section summarizes all known high-pressure structures with octahedrally-coordinated silicon. Excluded from this survey are several room-pressure silicon phosphates (Bissert and Liebau 1970, Liebau and Hesse 1971, Tillmanns et al. 1973,

Mayer 1974, Durif et al. 1976, Hesse 1979), as well as the crustal mineral thaumasite, which features an unusual $\text{Si}(\text{OH})_6$ polyhedron (Edge and Taylor 1971, Effenberger et al. 1983). The high-pressure $^{\text{VI}}\text{Si}$ silicates are conveniently subdivided into three groups:

Structures with all $^{\text{VI}}\text{Si}$

Above about 20 GPa, corresponding to the Earth's lower mantle, all silicates studied to date are observed to transform to one of ten different dense structure types in which all Si is six-coordinated (Table 1). Eight of these structures, including the rutile and the topologically related calcium chloride structures, perovskite-type structures, the ilmenite structure, hollandite-type structures, the calcium ferrite structure, the pyrochlore structure, and the K_2NiF_4 structure, are well known room-pressure topologies for

Table 1. Structures with all $^{\text{VI}}\text{Si}$.

<i>Formula</i>	<i>Name</i>	<i>Structure type</i>	<i>Reference</i>
SiO_2	Stishovite	Rutile	Stishov and Popova (1961)
SiO_2	-	CaCl_2	Tsuchida and Yagi (1989)
MgSiO_3	-	Perovskite	Liu (1974)
MgSiO_3	-	Ilmenite	Kawai et al. (1974)
KAlSi_3O_8	-	Hollandite	Kume et al. (1966)
$\text{NaAlSi}_3\text{O}_8$	-	CaFe_2O_4	Liu (1977c)
$\text{Sc}_2\text{Si}_2\text{O}_7$	-	Pyrochlore	Reid et al. (1977)
Ca_2SiO_4	-	K_2NiF_4	Liu (1978b)
$\text{MgSi}_2\text{O}_4(\text{OH})_2$	"Phase D"	New	Yang et al. (1997)
$\text{AlSiO}_3(\text{OH})$	"Phase egg"	New	Schmidt et al. (1998)

Table 2. Corner-linked framework structures with $^{\text{VI}}\text{Si}$ and $^{\text{IV}}\text{Si}$.

<i>Formula</i>	<i>Structure type</i>	<i>Reference</i>
CaSi_2O_5	Titanite	Angel (1997)
$\text{Mg}_3^{\text{VI}}(\text{MgSi})_2(^{\text{IV}}\text{Si}_3\text{O}_{12})$	Garnet (Majorite)	Fujino et al. (1986)
$\text{Na}_2^{\text{VI}}\text{Si}(^{\text{IV}}\text{Si}_2\text{O}_7)$	New	Fleet and Henderson (1995)
$\text{K}_2^{\text{VI}}\text{Si}(^{\text{IV}}\text{Si}_3\text{O}_9)$	Wadeite	Swanson and Prewitt (1983)
$\text{Ba}^{\text{VI}}\text{Si}(^{\text{IV}}\text{Si}_3\text{O}_9)$	Benitoite	Finger et al. (1995)
$\text{Ba}^{\text{VI}}\text{Si}(^{\text{IV}}\text{Si}_3\text{O}_9)$	BaGe_4O_9	Hazen et al. (1999)
$\text{Na}_6^{\text{VI}}\text{Si}_3(^{\text{IV}}\text{Si}_9\text{O}_{27})$	New	Fleet (1996)
$(\text{Na}_{1.8}\text{Ca}_{1.1})^{\text{VI}}\text{Si}(^{\text{IV}}\text{Si}_5\text{O}_{14})$	New	Gasparik et al. (1995)
$\text{Na}_8^{\text{VI}}\text{Si}(^{\text{IV}}\text{Si}_6\text{O}_{18})$	New	Fleet (1998)

Table 3. Other structures with mixed $^{\text{VI}}\text{Si}$ and $^{\text{IV}}\text{Si}$.

<i>Formula</i>	<i>Name</i>	<i>Structure type</i>	<i>Reference</i>
$\text{Mg}_{14}\text{Si}_5\text{O}_{24}$	Anhydrous Phase B	$\text{Mg}_{14}\text{Ge}_5\text{O}_{24}$	Finger et al. (1989)
$\text{Mg}_{12}\text{Si}_4\text{O}_{19}(\text{OH})_2$	Phase B	New	Finger et al. (1989)
$\text{Mg}_{10}\text{Si}_3\text{O}_{14}(\text{OH})_4$	Superhydrous B	New	Pacalo & Parise (1992)
$\text{Na}^{\text{VI}}(\text{Mg}_{0.5}\text{Si}_{0.5})^{\text{IV}}\text{Si}_2\text{O}_6$	-	Pyroxene	Angel et al. (1988)
$(\text{Mg,Fe})_2\text{SiO}_4$	Ringwoodite	Spinel	Jackson et al. (1974)

transition-metal oxides. In the high-pressure silicate isomorphs, silicon occupies the octahedral transition metal site, while other cations may adopt six or greater coordination. The other two $^{\text{VI}}\text{Si}$ structures are the new, dense hydrous compounds $\text{MgSi}_2\text{O}_4(\text{OH})_2$ (“phase D”) and $\text{AlSiO}_3(\text{OH})$ (“phase egg”).

- (1) *Corner-linked framework structures with mixed $^{\text{IV}}\text{Si}$ and $^{\text{VI}}\text{Si}$* : At pressures between about 5 and 20 GPa some silicates form with mixed four and six coordination. One distinctive group of at least 9 structure types is characterized by a three-dimensional, corner-linked framework of silicate octahedra and tetrahedra (Table 2).
- (2) Other structures with mixed $^{\text{IV}}\text{Si}$ and $^{\text{VI}}\text{Si}$: Other mixed-coordination silicates include varieties of the well known pyroxene and spinel structures, as well as complex new magnesium-bearing phases designated superhydrous B, phase B, and anhydrous phase B (Table 3).

The rutile structure. Stishovite, a form of SiO_2 synthesized above ~ 10 GPa, represents the stable form of free silica throughout much of the Earth’s mantle, to a depth of ~ 1500 km (Hemley et al. 1995). In addition to its assumed role in mantle mineralogy, stishovite has elicited considerable interest as a product of the transient high-pressure, high-temperature environments of meteorite impacts (Chao et al. 1962). The discovery of stishovite grains in sediments near the Cretaceous-Tertiary boundary layer (McHone et al. 1989) has provided support for the hypothesis that a large impact, rather than volcanism, led to a mass extinction approximately 65 million years ago.

Stishovite has the tetragonal rutile (TiO_2) structure, with edge-linked chains of SiO_6 octahedra that extend parallel to the c axis and octahedra corner linked to four adjacent chains (Fig. 1a). Two symmetrically distinct atoms—Si at $(0, 0, 0)$ and O at $(x, x, 0)$ with x approximately 0.3—define the structure in space group $P4_2/mnm$.

The first stishovite structure refinements were obtained by powder diffraction on small synthetic samples (Stishov and Belov 1962, Preisinger 1962, Baur and Khan 1971, see also Stishov 1995). A much-improved refinement was presented by Sinclair and Ringwood (1978), who synthesized single crystals up to several hundred microns. Subsequent single-crystal structure studies by Hill et al. (1983) under room conditions and by Sugiyama et al. (1987) and Ross et al. (1990) at high pressure, amplify the earlier work.

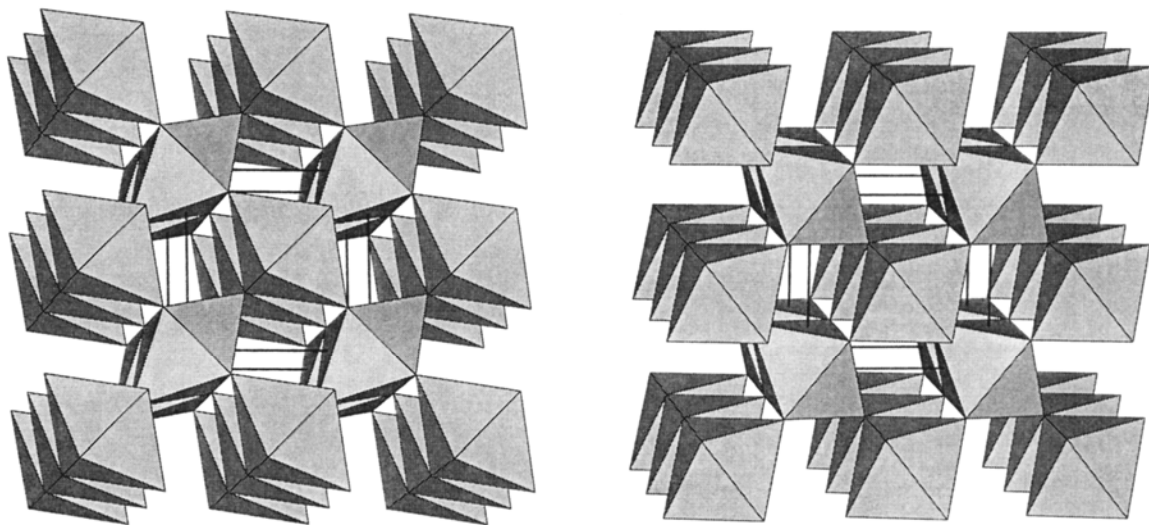


Figure 1. (a) Crystal structure of stishovite, SiO_2 . (b) Crystal structure of calcium-chloride-type SiO_2 .

The calcium chloride structure. Above ~60 GPa, stishovite transforms reversibly to the orthorhombic calcium chloride (CaCl_2) structure, based on high-pressure X-ray diffraction (Tsuchida and Yagi 1989) and Raman spectroscopy (Kingma et al. 1995). The nonquenchable calcium chloride structure of SiO_2 is topologically identical to the rutile structure (e.g. Hemley and Cohen 1992); the two differ only by a slight rotation of octahedral chains (Fig. 1b).

Perovskite structures. Perovskite structures include dozens of topologically related forms with the general formula ABX_3 , where A and B are cations and X is an anion. The dominant structural feature is a three-dimensional array of corner-linked BX_6 octahedra. Each octahedron is thus linked to six others, and A cations occupy interstices defined by eight octahedra (Fig. 2). Remarkable structural diversity is achieved by tilting and distortion of octahedra, as well as cation ordering, offsets from centric cation positions, and cation and anion nonstoichiometry (Glazer 1972, Megaw 1973, Hazen 1988).

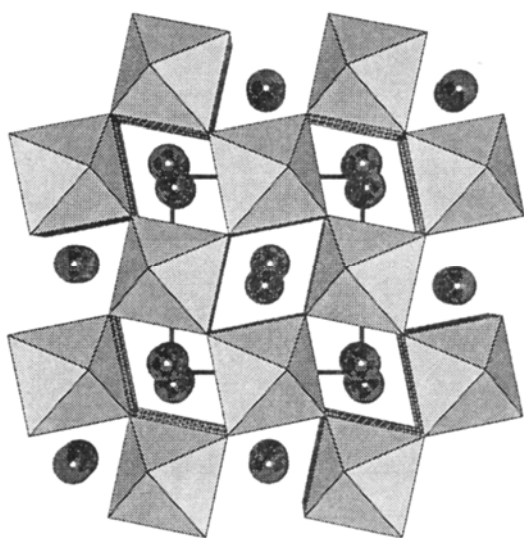


Figure 2. The crystal structure of perovskite-type MgSiO_3 .

High-pressure synthesis and structural description of silicate perovskites have posed significant challenges to earth scientists since Ringwood (1962, 1966) originally suggested the existence of perovskite forms of MgSiO_3 and CaSiO_3 . High-pressure transformations from pyroxene and garnet structures to perovskite in the analogous systems $\text{Ca}(\text{Ge},\text{Si})\text{O}_3$ and $\text{Ca}(\text{Ti},\text{Si})\text{O}_3$ (Marezio et al. 1966, Ringwood and Major 1967a, 1971; Reid and Ringwood 1975) supported this hypothesis. Pure silicate perovskites were first produced at the Australian National University (Liu 1974, 1975a,b; 1976a,b,c; Liu and Ringwood 1975) and results were quickly duplicated in Japan and the United States (Sawamoto 1977, Ito 1977, Ito and Matsui 1977, 1978, 1979; Mao et al 1977). These workers demonstrated that above pressures of about 25 GPa many silicates transform to an orthorhombic perovskite structure, in which silicon octahedra form a three-dimensional corner-linked network, while larger cations fill positions with oxygen coordination of eight or greater. By the late 1970s many earth scientists were persuaded that the Earth's 670-km seismic discontinuity, which divides the transition zone from the lower mantle, coincides with a perovskite phase-transition boundary, and that perovskite of approximate composition $(\text{Mg}_{0.9}\text{Fe}_{0.1})\text{SiO}_3$ is a dominant lower mantle mineral (Anderson 1976, Liu 1977a, 1979; Yagi et al. 1978).

The simplest perovskite variant is the cubic form (space group $P4/m\bar{3}2/m$, represented by CaSiO_3 , which is stable above about 15 GPa. This phase, first synthesized by Liu and Ringwood (1975), has a structure that is completely specified by the cubic cell edge, a , because all atoms are in invariant special positions. The Si- and O-atom positions, for example, are $(0, 0, 0)$ and $(1/2, 0, 0)$, respectively, so the Si-O distance of the regular silicon octahedron is $a/2$. Similarly, the octahedral volume is $a^3/6$. Calcium silicate perovskite cannot be quenched metastably to room pressure; samples invariably transform to glass upon release of pressure. Nevertheless, equation-of-state measurements of CaSiO_3 by Mao et al., (1989) to 134 GPa define the structure as a

function of pressure and allow reasonable extrapolation to room-pressure values.

The corner-linked silicate perovskite framework will tilt to accommodate divalent cations smaller than Ca. Thus, the structure of (Mg,Fe)SiO₃, widely thought to be the Earth's most abundant mineral, is orthorhombic (space group *Pbnm*). Silicon occupies near-regular octahedral coordination, while magnesium is in a larger site with eight nearest-neighbor O atoms. Orthorhombic cell parameters possess a $2\sqrt{2} \times 2\sqrt{2} \times 2$ relationship to the simple cubic axes. Initial studies of this structure were performed by Yagi et al. (1978, 1982) and Ito and Matsui (1978) on powders. Subsequent synthesis by Ito and Weidner (1986) of single crystals led to much more precise structure refinements under room conditions (Horiuchi et al. 1987) and at high pressure (Kudoh et al. 1987, Ross and Hazen 1990).

Octahedral tilt transitions could lead to a number of other tetragonal, orthorhombic, or monoclinic structural variants of silicate perovskites (e.g. Hemley and Cohen 1992). All silicate perovskite structure studies based on X-ray diffraction indicate complete ordering of Si and the divalent cations in the octahedral sites and the larger sites, respectively. Iron-bearing silicate perovskites, however, always contain significant Fe³⁺ (Fei et al. 1996, Mao et al. 1997, McCammon 1997, 1998), which suggests that trivalent cations may occupy both cation sites, as it does in the high-pressure perovskite form of Fe₂O₃ (Olsen et al. 1991). Much work remains to be done on the compositional limits, structural variants, stability, and phase transitions in silicate perovskites.

The ilmenite structure. The ilmenite (FeTiO₃) and corundum (α -Al₂O₃) structures have long been recognized as likely candidates for high-pressure silicates in which all cations assume octahedral coordination (J. B. Thompson, as quoted in Birch 1952). These two structures are topologically identical, and differ only in the lack of ordered cations in corundum (Fig. 3). Ringwood and Seabrook (1962) demonstrated such a transformation in the germanate analog, MgGeO₃, and other high-pressure germanate isomorphs were soon identified. The silicate end member MgSiO₃ was subsequently produced by Kawai et al. (1974) and this material was identified by Ito and Matsui (1974) as having the ilmenite ($R\bar{3}$) structure, in which silicon and magnesium must be at least partially ordered. Natural (Mg,Fe)SiO₃ ilmenite was recently identified in shocked meteorites by Sharp et al. (1997) and Tomioka and Fujino (1997), and has provisionally been named akimotoite.

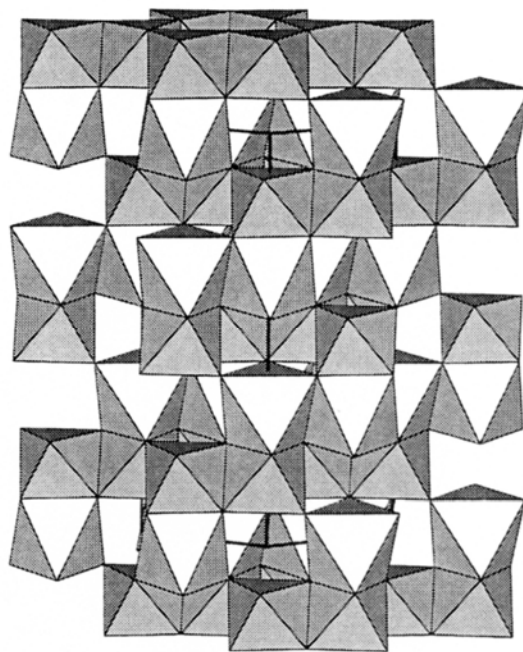


Figure 3. The crystal structure of ilmenite-type MgSiO₃.

Horiuchi et al. (1982) synthesized single crystals of MgSiO₃ ilmenite and documented details of the crystal structure. Silicon and magnesium appear to be almost completely ordered in the two symmetrically distinct cation positions. Silicate ilmenites are unique in that each silicon octahedron shares a face with an adjacent magnesium

octahedron—no other known silicate structure displays face sharing between a silicon polyhedron and another tetrahedron or octahedron. Magnesium-silicon ordering may be facilitated by this feature, for only in a completely ordered silicate ilmenite can face sharing between two silicate octahedra be avoided.

The stability of silicate ilmenites is quite restricted, in terms of both pressure and composition. Pressures above 20 GPa are required to synthesize the MgSiO_3 phase, but above ~ 25 GPa perovskite forms instead (Fei et al. 1990). Addition of more than a few atom percent iron for magnesium stabilizes the perovskite form at the expense of ilmenite; 10% iron completely eliminates the ilmenite field. Of the other common divalent cations, only zinc has been found to form a stable silicate ilmenite— ZnSiO_3 (Ito and Matsui 1974, Liu 1977b).

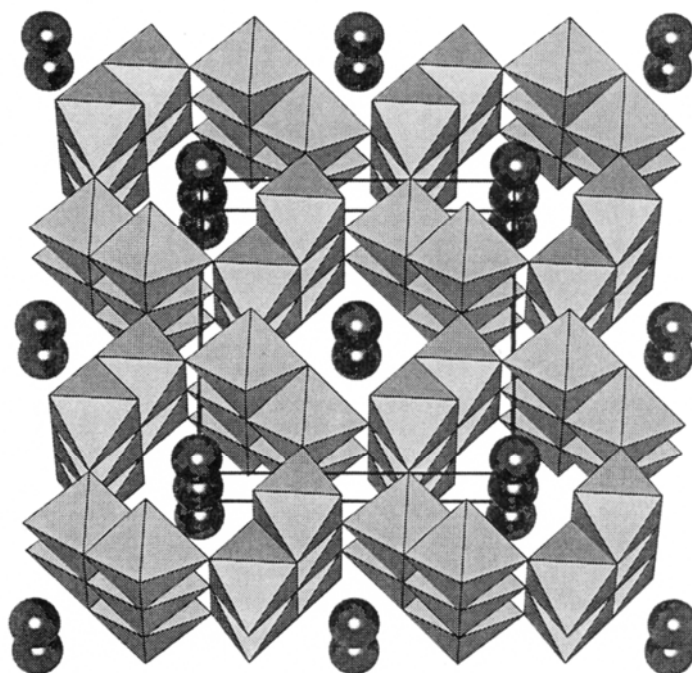


Figure 4. The hollandite-type crystal structure.

Hollandite structures. Feldspars, including KAlSi_3O_8 , $\text{NaAlSi}_3\text{O}_8$, and $\text{CaAl}_2\text{Si}_2\text{O}_8$, are the most abundant minerals in the Earth's crust. Accordingly, a number of researchers have examined high-pressure phase relations for these minerals (Kume et al. 1966, Ringwood et al. 1967, Reid and Ringwood 1969, Kinomura et al. 1975, Liu 1978a, 1978b; Yagi et al. 1994). All of these investigators concluded that feldspars ultimately transform to the hollandite ($\text{BaMn}_8\text{O}_{16}$) structure at pressures above ~ 10 GPa. Hollandite-type silicates have thus been proposed as a possible repository for alkali metals in the Earth's mantle. Further support for this hypothesis is provided by Gillet et al. (2000), who identified natural $\text{NaAlSi}_3\text{O}_8$ hollandite in the shocked Sixiangkou meteorite.

The ideal hollandite structure is tetragonal, $I4/m$, with double chains of edge-sharing (Si,Al) octahedra (Fig. 4). The relatively large alkali or alkaline-earth cations occupy positions along large channels that run parallel to c . However, as in the perovskite structure, lower-symmetry variants of the hollandite structure result from structural distortions, cation ordering, and cation off-centering.

Yamada et al. (1984) refined the structure of KAlSi_3O_8 hollandite from powder diffraction data. They detected no deviations from tetragonal symmetry and so assumed

complete disorder of aluminum and silicon on the one symmetrically distinct octahedral site. Natural hollandites, however, are typically monoclinic (pseudotetragonal) owing to ordering of Mn^{3+} and Mn^{4+} or other octahedral cations, as well as distortion of the channels. Zhang et al. (1993) obtained single crystals of KAlSi_3O_8 hollandite; they refined the structure at several pressures to 4.5 GPa and confirmed that Si and Al are disordered among octahedral sites.

Gasparik (1989) inadvertently synthesized single crystals of lead aluminosilicate hollandite ($\text{Pb}_{0.8}\text{Al}_{1.6}\text{Si}_{2.4}\text{O}_8$) at 16.5 GPa and 1450°C, while employing a PbO flux in studies of the Na-Mg-Al-Si system. Downs et al. (1995) subsequently described the crystal chemistry of this phase. They found that off-centering of Pb atoms leads to a reduction in symmetry to $I4$, but Al and Si are disordered on the one symmetrically distinct octahedral site.

A number of other silicate hollandites have been synthesized but not fully characterized by X-ray diffraction. Reid and Ringwood (1969) made hollandites with compositions approximating $\text{SrAl}_2\text{Si}_2\text{O}_8$ and $\text{BaAl}_2\text{Si}_2\text{O}_8$ (though reported alkaline-earth contents are significantly less than 1.0), while Madon et al. (1989) described synthesis of $(\text{Ca}_{0.5}\text{Mg}_{0.5})\text{Al}_2\text{Si}_2\text{O}_8$ hollandite. Given the 1:1 ratio of aluminum to silicon in these samples, ordering of Al and Si into symmetrically distinct octahedra is possible, though structure-energy calculations by Post and Burnham (1986) suggest that octahedral cations are disordered in most hollandites. This proposition is supported by Vicat et al.'s (1986) ordering studies of synthetic hollandite ($\text{K}_{1.33}\text{Mn}^{4+}_{6.67}\text{Mn}^{3+}_{1.33}\text{O}_{16}$), which displays diffuse diffraction effects characteristic of some short-range order, but long-range disorder of Mn^{4+} and Mn^{3+} .

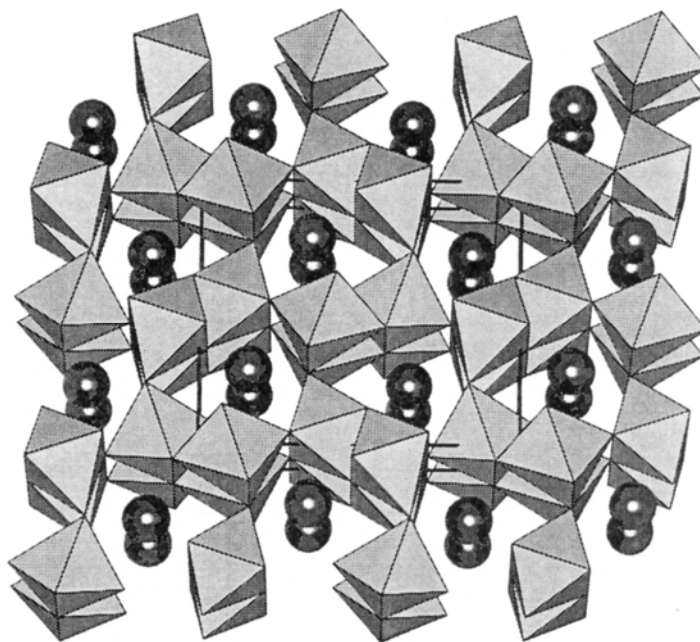


Figure 5. The calcium ferrite-type crystal structure.

The calcium ferrite structure. High-pressure studies of NaAlGeO_4 (Ringwood and Major 1967a, Reid et al. 1967) and NaAlSiO_4 (Liu 1977c, 1978a; Yamada et al. 1983) revealed that these compounds adopt the orthorhombic calcium ferrite (CaFe_2O_4) structure in which all Si and Al are in octahedral coordination (Fig. 5). Yamada et al. (1983), who synthesized NaAlSiO_4 at pressures above 24 GPa, used X-ray diffraction to identify their polycrystalline product and propose atomic coordinates. The basic topology

of the high-pressure NaAlSiO_4 structure is thus well established. Bond distances calculated from their refined coordinates, however, yield unreasonably short cation-oxygen distances, so details of the structure remain in doubt.

The calcium ferrite structure bears a close relationship to hollandite (Yamada et al. 1983). Both structures consist of double octahedral chains which are joined to form 'tunnels' parallel to c that accommodate the alkali or alkaline-earth cations. In hollandite four double chains form square tunnels, whereas in calcium ferrite four chains define triangular tunnels.

The pyrochlore structure. Thortveitite ($\text{Sc}_2\text{Si}_2\text{O}_7$) contains Si_2O_7 groups and Sc in distorted octahedral coordination. The structure is unusual in that the Si-O-Si linkage is constrained to be collinear because the O atom lies on a center of inversion. Reid et al. (1977) studied high-pressure transformations of $\text{Sc}_2\text{Si}_2\text{O}_7$ and its isomorph, $\text{In}_2\text{Si}_2\text{O}_7$, from the thortveitite structure to the pyrochlore structure at 12 GPa and 1000°C. They report structures based on powder X-ray diffraction data from these two high-pressure compounds.

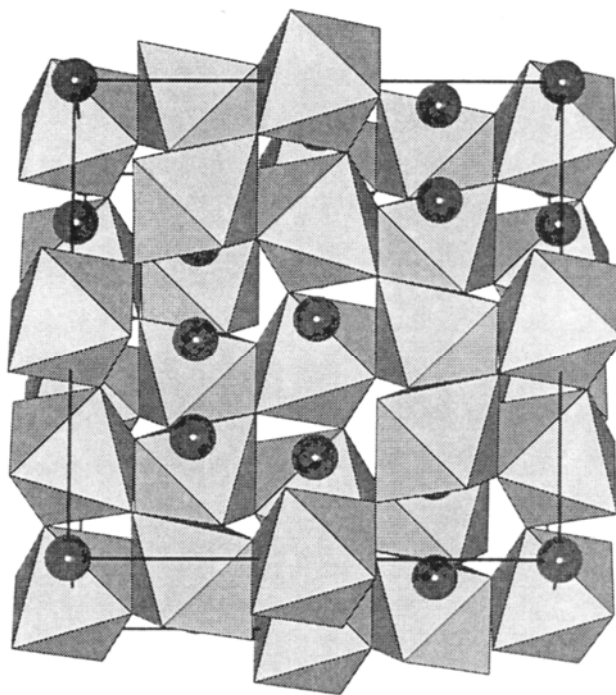


Figure 6. The pyrochlore-type crystal structure.

The cubic pyrochlore structure (space group $Fd\bar{3}m$) contains four independent atoms with only one variable positional parameter, the x coordinate of O2 (Fig. 6). It features silicon in an octahedral framework corner-linked by O2, with scandium in distorted cubic eight coordination corner-linked by O1. The increase in coordination number of both cations, from 4 and 6 in thortveitite to 6 and 8 in pyrochlore, leads to a significant density increase, from 3.30 g/cm^3 in thortveitite to 4.28 g/cm^3 in the high-pressure phase.

The potassium nickel fluoride structure. The potassium nickel fluoride structure (K_2NiF_4), in which K and Ni are nine- and six-coordinated respectively, is well known among transition-metal oxides such as Sr_2TiO_4 . Reid and Ringwood (1970) proposed K_2NiF_4 as a possible high-pressure silicate structure following their synthesis of Ca_2GeO_4 . Liu (1978b) synthesized a high-pressure polymorph of Ca_2SiO_4 at 22 to 26

GPa and 1000°C and recognized the distinctive tetragonal cell $a = 3.564(3)$, $c = 11.66(1)$ Å as characteristic of the K_2NiF_4 structure. Liu recorded 25 powder diffraction lines consistent with this unit cell, although structural details of the high-pressure calcium silicate were not provided.

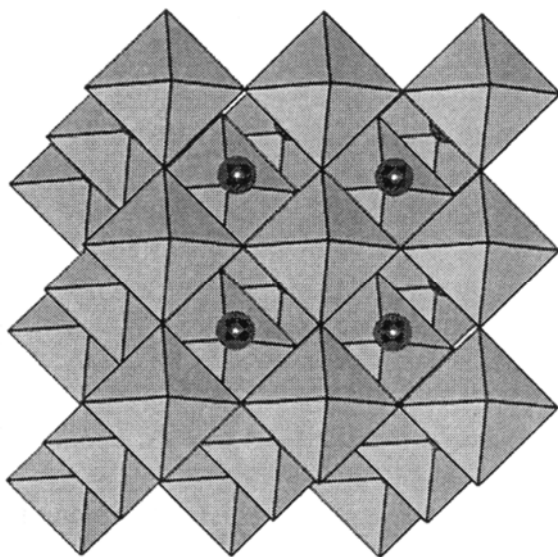


Figure 7. The K_2NiF_4 -type crystal structure.

topology. Additional studies of Ca_2SiO_4 will be required to resolve the exact nature of this high-pressure phase.

New hydrous magnesium silicate (“Phase D”). Yang et al. (1997) determined the novel structure of the dense hydrous magnesium silicate phase D, $Mg_{1.11}Si_{1.89}H_{2.22}O_6$ (ideal formula $MgSi_2O_4(OH)_2$), which was synthesized at 20 GPa and 1200°C. This material was originally identified by Liu (1986, 1987) based on powder diffraction patterns, and was termed “phase D,” in keeping with the standard nomenclature for new synthetic hydrous magnesium silicates. The trigonal structure (space group $P\bar{3}1m$; Fig. 8) features gibbsite-like dioctahedral sheets of edge-linked silicate octahedra (i.e., an ordered octahedral sheet with two of every three sites occupied). MgO_6 octahedra are located above and below each vacant octahedral site in the Si layer. The O-H bonding occurs exclusively between silicate octahedral layers.

Yang et al. (1997) note that this phase, which is the only known hydrous magnesium silicate with no ^{IV}Si , is also the densest ($\rho = 3.50 \text{ g/cm}^3$).

New hydrous aluminosilicate (“phase egg”). Schmidt et al. (1998) solved the structure of $AlSiO_3(OH)$, a high-pressure phase first described by Eggleton et al. (1978), and subsequently dubbed “phase egg.” Polycrystalline material was synthesized by

The aristotype structure with K_2NiF_4 topology is tetragonal, space group $I4/mmm$, with four atoms in the asymmetric unit and only two variable positional parameters (Fig. 7). Octahedrally coordinated Ni (or Si) at the origin is coordinated to four F1 (or O1) at $(0, 1/2, 0)$ and two F2 (or O2) at $(0, 0, z)$. Four Ni-F1 (or Si-O1) bond distances are exactly $a/2$ and all adjacent F-Ni-F (or O-Si-O) angles are 90° .

Slight distortions of the $I4/mmm$ structure lead to a number of subgroups of lower-symmetry variants (Hazen 1990). These topologically identical structures have received much attention, because the first of the so-called “high-temperature” copper oxide superconductor, $(La,Ba)_2CuO_4$, adopts the K_2NiF_4

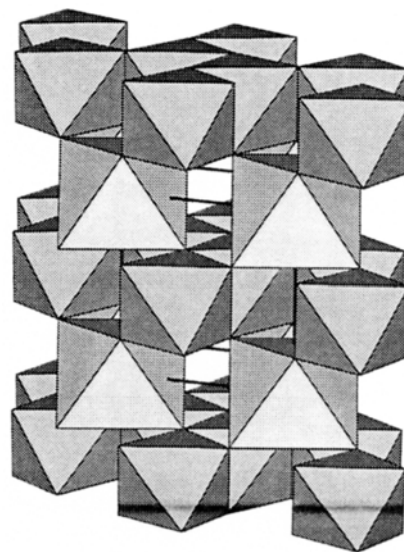


Figure 8. The crystal structure of phase D.

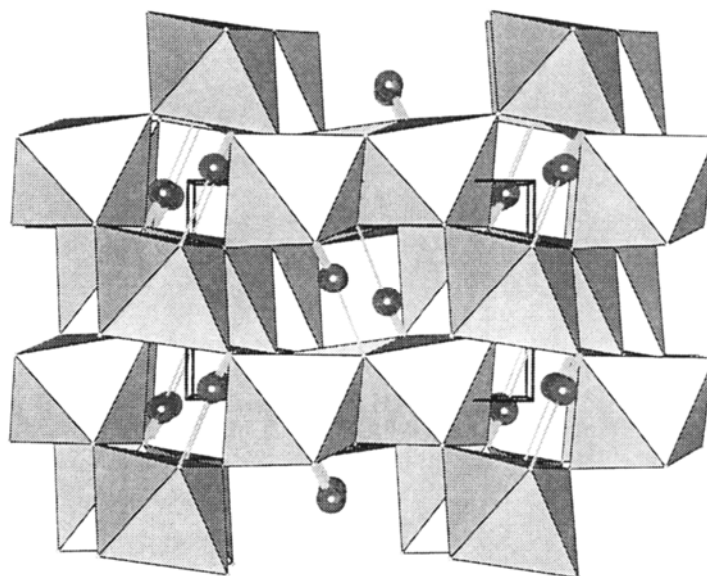


Figure 9. The crystal structure of “Phase egg.”

Schmidt (1995) at pressures above 7 GPa and temperatures above 700°C. The novel monoclinic structure (space group $P2_1/n$) is closely related to that of stishovite. As in stishovite, the structure consists of edge-sharing octahedral columns that are linked by octahedral corner sharing (Fig. 9). In this hydrous phase, however, the columns are offset every four octahedra so that each SiO_6 octahedron shares edges with one $^{\text{IV}}\text{Si}$ and two $^{\text{VI}}\text{Al}$, while each AlO_6 octahedron shares edges with two $^{\text{IV}}\text{Si}$ and one $^{\text{VI}}\text{Al}$. Hydrogen atoms occupy sites in the structural channels.

Corner-linked framework silicates with mixed $^{\text{IV}}\text{Si}$ and $^{\text{VI}}\text{Si}$

One of the most fascinating aspects of the Earth’s transition zone is the appearance of a group of high-pressure silicates with both $^{\text{IV}}\text{Si}$ and $^{\text{VI}}\text{Si}$. The stability of these minerals is apparently confined to a rather narrow pressure range from approximately 5 to 20 GPa. Within these limits, however, are silicate structures of remarkable complexity and great topological interest. In this section we consider a diverse subset of these mixed IV-VI silicates—structures based on corner-linked silicate frameworks.

High-pressure framework silicates with mixed $^{\text{IV}}\text{Si}$ and $^{\text{VI}}\text{Si}$ were systematized by Hazen et al. (1996), who tabulated eight phases that can be represented by the structural formula $(A^{1+}_{4-2x}B^{2+}_x)^{\text{VI}}\text{Si}_m(^{\text{IV}}\text{Si}_n\text{O}_{2(m+n)+2})$, where x , m , and n specify the amounts of alkaline earth cations, six-coordinated silicon, and four-coordinated silicon, respectively. This structural formula is normalized to a total formal charge of +4 for alkali plus alkaline earth cations. Given that constraint, values of m and n restrict the topology of the silicate polyhedral array. The special case of $m = 0$ (all $^{\text{IV}}\text{Si}$) includes numerous low-pressure framework silicates, such as feldspars, feldspathoids, and zeolites. Corner-linked silicate frameworks with $n = 0$ (all $^{\text{VI}}\text{Si}$) include the perovskite and pyrochlore structures, reviewed in the previous section.

All of the known IV-VI frameworks (with nonzero m and n) incorporate either individual SiO_6 octahedra or corner-sharing $n\text{SiO}_5$ chains of octahedra. These network-forming modules are cross-linked by a variety of tetrahedral modules, including individual SiO_4 tetrahedra, Si_2O_7 dimers, and larger tetrahedral rings and layers. In a fully connected 3-D network, all oxygen atoms are bridging; each oxygen links two Si polyhedra. In a fully-linked IV-VI framework, therefore, the number of exposed oxygen

atoms (those not bonded to two octahedra) on octahedral modules must equal the number of exposed oxygen atoms (those not bonded to two tetrahedra) on tetrahedral modules. Thus, for example, in the $(\text{Na}_2\text{Ca})\text{Si}_2(\text{Si}_3\text{O}_{12})$ garnet framework, individual SiO_6 octahedra must be linked to individual SiO_4 tetrahedra in a 2:3 ratio; each octahedron links to six tetrahedra, and each tetrahedron links to four octahedra. Similarly, equal numbers of isolated SiO_6 octahedra and Si_3O_9 tetrahedral rings (both with six exposed oxygen atoms per module) form a 3-D framework in the wadeite-type, benitoite-type, and barium germanate-type structures.

The known IV-VI framework silicate structures are reviewed below.

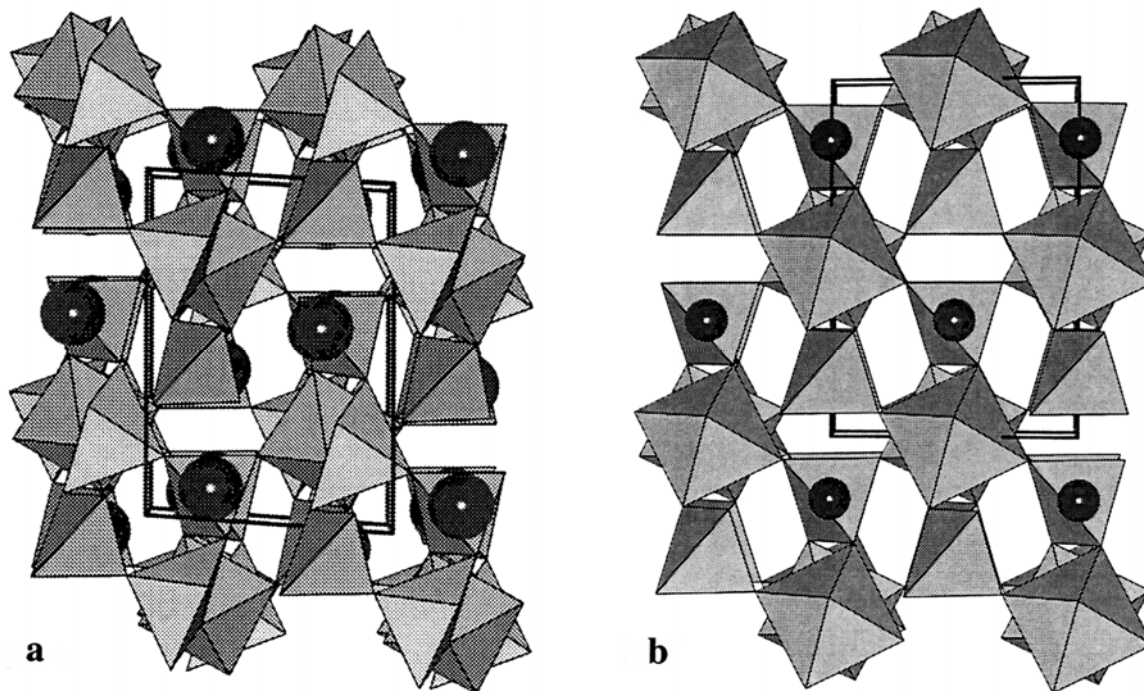


Figure 10. (a) The titanite-related crystal structure of CaSi_2O_5 (space group $I\bar{1}$). (b) The titanite-type structure of CaSi_2O_5 at high pressure (space group $A2/a$).

Titanite-related structures ($m = 2$; $n = 2$). Titanite or sphene, CaTiSiO_5 , is monoclinic (aristotype space group $A2/a$) and features a corner-linked framework of Ti octahedra and Si tetrahedra. Finger and Hazen (1991) proposed that a silicate analog, CaSi_2O_5 , or $\text{Ca}_2^{\text{VI}}\text{Si}_2^{\text{IV}}\text{Si}_2\text{O}_{10}$ in terms of the general formula cited above, should adopt the titanite structure at high pressure. Such a calcium silicate, isostructural with the previously described CaGe_2O_5 (Nevskii et al. 1979a), would incorporate corner-sharing chains of silicate octahedra like those in perovskite and stishovite, but these chains would be cross-linked by individual silicate tetrahedra. Stebbins and Kanzaki (1991) and Kanzaki et al. (1991) conducted synthesis experiments in the CaSiO_3 system and tentatively identified a high-pressure, titanite-related isomorph of composition CaSi_2O_5 , based on ^{29}Si NMR.

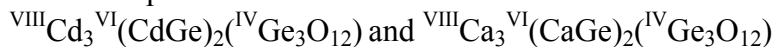
Single crystals of this high-pressure form of CaSi_2O_5 were subsequently synthesized by Angel et al. (1996) at 11 GPa and 1350°C and quenched to room conditions. They found that at room pressure this material adopts an unusual distorted titanite structure (triclinic, space group $I\bar{1}$; Fig. 10a), in which silicon occurs in 4-, 5-, and 6-coordination—the only known inorganic phase with 5-coordinated Si. Angel et al. found

that the 5-coordinated site is a square pyramid with an average Si-O distance of 1.73 Å, compared to the 1.80 Å distance typical of silicate octahedra. The sixth oxygen, which would normally complete this octahedron in titanite, is tilted away from the 5-coordinated polyhedron due to the mismatch of polyhedra in the room-pressure structure.

Angel (1997) further examined these crystals at high pressure and observed a first-order transition, accompanied by a 2.9% volume reduction, to the monoclinic ($A2/a$) titanite structure (Fig. 10b). Single crystals are preserved through this largely displacive transition. Angel found that the monoclinic structure, once formed at pressures above about 0.2 GPa, can be quenched and preserved as single crystals at room pressure. Subsequent synthesis experiments by Kubo et al. (1997) and Knoche et al. (1998) have demonstrated a complete solid solution between titanite and the CaSi_2O_5 end member. At room pressure and temperature the titanate end member has lower monoclinic symmetry (space group $P2_1/a$), as a result of offsets of Ti atoms from centric positions. Knoche et al. (1998) note that as little as 10% Si substitution for Ti is sufficient to suppress this effect and produce the maximal $A2/a$ symmetry.

The garnet structure ($m = 2$; $n = 3$). Garnets are common crustal silicates of the general formula $^{\text{VIII}}A_3^{\text{VI}}B_2(\text{IVSi}_3\text{O}_{12})$, where eight-coordinated A is commonly Mg, Fe, Mn or Ca and six-coordinated B is usually Fe, Al or Cr. The structure may be viewed as a corner-linked framework of alternating Si^{4+} tetrahedra and trivalent octahedra. This framework defines eight-coordinated sites that accommodate divalent cations. The ideal garnet structure is cubic (space group $Ia\bar{3}d$), with only four symmetry-independent atoms: A , B , Si and O.

Ringwood and Major (1967a) and Prewitt and Sleight (1969) demonstrated that germanate garnets of compositions



form because Ge^{4+} plus a divalent cation can substitute for the trivalent B cation. These garnets are topologically identical to the cubic aristotype, but ordering of octahedral B cations yields a tetragonal garnet of symmetry group lower than the $Ia\bar{3}d$ form. Ringwood and Major (1967a) were the first to synthesize a high-pressure silicate garnet, MnSiO_3 , which Akimoto and Syono (1972) subsequently indexed as tetragonal. High-pressure silicate garnets thus incorporate silicon in both four and six coordination.

The significance of these synthetic samples has been enhanced by discovery of natural high-pressure garnets with $^{\text{VI}}\text{Si}$. Smith and Mason (1970) described a natural silica-rich garnet from the Coorara meteorite. The composition of this mineral, which they named majorite, is $^{\text{VIII}}(\text{Mg}_{2.86}\text{Na}_{0.10}\square_{0.14})^{\text{VI}}(\text{Fe}_{0.97}\text{Al}_{0.22}\text{Cr}_{0.03}\text{Si}_{0.78})^{\text{IV}}\text{Si}_3\text{O}_{12}$. Haggerty and Sautter (1990) discovered mantle-derived nodules with silica-rich garnet of composition of more than four Si atoms per twelve O atoms (as opposed to three Si in crustal garnets). These observations led the authors to propose that the nodules originated from a depth greater than 300 km.

Single crystals of MnSiO_3 garnet were first synthesized by Fujino et al. (1986), who determined the space group to be tetragonal ($I4_1/a$; Fig. 11). Mn and Si atoms were found to be fully ordered in two symmetrically distinct octahedral sites. At pressures above 15 GPa and temperatures greater than about 1973 K, MgSiO_3 forms the garnet $^{\text{VIII}}\text{Mg}_3^{\text{VI}}(\text{MgSi})_2(\text{IVSi}_3\text{O}_{12})$ —the same composition as the silicate ilmenites and perovskites described above. Angel et al. (1989) synthesized single crystals of this phase and determined the crystal structure. In that sample, octahedral Mg and Si were slightly disordered, yielding an M1 site composition of $(\text{Si}_{0.8}\text{Mg}_{0.2})$. Heinemann et al. (1997) and

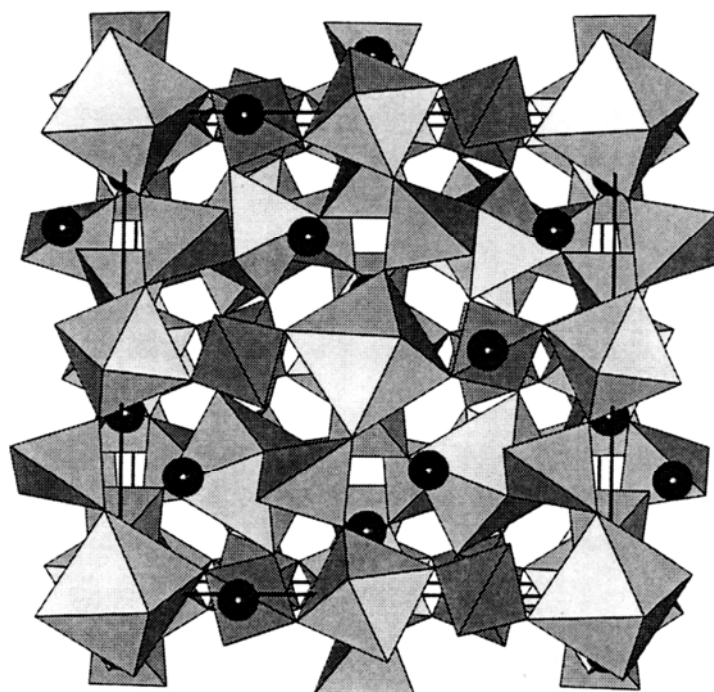


Figure 11. The crystal structure of garnet-type MgSiO_3 .

Nakatsuka et al. (1999a) subsequently documented the structures of garnets on the pyrope-majorite join ($\text{Mg}_3\text{Al}_2\text{Si}_3\text{O}_{12}$ - $\text{Mg}_3(\text{MgSi})\text{Si}_3\text{O}_{12}$) and observed the transition from cubic to tetragonal symmetry at intermediate compositions.

Of special note are high-pressure syntheses of garnets in the Na-Ca-Mg-Al-Si system, including sodium-calcium garnet $(\text{Na}_2\text{Ca})\text{Si}_2(\text{Si}_3\text{O}_{12})$ at 18 GPa and 1000°C by Ringwood and Major (1971). Subsequent work by Gasparik (1989, 1990) has yielded a variety of IV-VI silicates, including the sodium-magnesium garnet, $(\text{Na}_2\text{Mg})\text{Si}_2(\text{Si}_3\text{O}_{12})$. In these garnets all octahedral and tetrahedral sites are occupied by Si, thus forming a continuous silicate framework with no requirement for octahedral ordering. Accordingly, Hazen et al. (1994a) determined that the sodium-magnesium phase possesses the ideal cubic garnet structure, though the complete structure has not yet been published.

Studies of majoritic garnets with more complex compositions are revealing a variety of cation ordering schemes. For example, synthetic calcium-bearing majorite, $(\text{Ca}_{0.49}\text{Mg}_{2.51})(\text{MgSi})(\text{Si}_3\text{O}_{12})$, is tetragonal, with cation ordering on both octahedral (Mg-Si) and dodecahedral (Mg-Ca) sites (Hazen et al. 1994b). Nakatsuka et al. (1999b), on the other hand, refined the structure of a birefringent synthetic Cr-bearing majorite, $\text{Mg}_3(\text{Mg}_{0.34}\text{Si}_{0.34}\text{Al}_{0.18}\text{Cr}_{0.14})_2(\text{Si}_3\text{O}_{12})$, in which the Cr and other octahedral cations are evidently disordered between the two nonequivalent octahedral sites of the tetragonal structure.

New sodium trisilicate structure ($m = 2$; $n = 4$). Fleet and Henderson (1995) described the new structure of sodium trisilicate, $\text{Na}_2^{\text{VI}}\text{Si}^{\text{IV}}(\text{Si}_2\text{O}_7)$, which is monoclinic (space group $C2/c$; Fig. 12). Single crystals were synthesized at 9 GPa and 1200°C from a bulk composition of $\text{Na}_2\text{Si}_2\text{O}_5$. The corner-linked silicate framework is formed from alternating Si_2O_7 dimers and isolated silicate octahedra. Note that both of the structural modules—the tetrahedral dimer and isolated octahedron—have six exposed oxygens, so each module is linked to six of the other type. Sodium cations are in irregular six-coordination in structural channels.

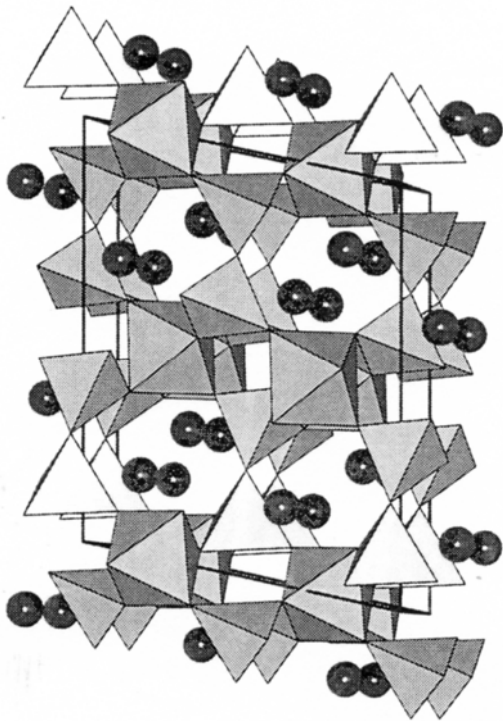


Figure 12. The crystal structure of a new sodium trisilicate.

coordination. Each bridging O1 atom is coordinated to two $^{\text{VI}}\text{Si}$ and two K, while O2 atoms are linked to one $^{\text{IV}}\text{Si}$, one $^{\text{VI}}\text{Si}$ and two K. Swanson and Prewitt (1983) synthesized single crystals of $\text{K}_2\text{Si}_4\text{O}_9$ in a piston-cylinder apparatus at ~ 4 GPa and 900°C . Their structure refinement confirmed the wadeite structure type and provided details of the extremely regular silicon octahedral environment.

The benitoite structure ($m = 2$; $n = 6$). Finger et al. (1995) described a high-pressure form of $\text{Ba}^{\text{VI}}\text{Si}^{\text{IV}}\text{Si}_3\text{O}_9$ with the benitoite ($\text{BaTiSi}_3\text{O}_9$) structure (hexagonal, space group $P\bar{6}c2$; Fig. 14). Samples were synthesized by Fursenko (1997) from oxides at 4 GPa and 1000°C and ground prior to studies by Rietveld powder diffraction methods. The structure, like that of wadeite, features a corner-linked framework in which three-member tetrahedral rings are linked to six isolated silicate octahedra, while each octahedron is linked to six three-member rings. Six-coordinated Ba cations occupy channels in this framework.

The barium germanate structure ($m = 2$; $n = 6$). Hazen et al. (1999) determined that single crystals of $\text{Ba}^{\text{VI}}\text{Si}^{\text{IV}}\text{Si}_3\text{O}_9$ synthesized at 4 GPa and 1000° are isostructural with barium tetragermanate (trigonal, space group $P3$; Fig. 15). This barium germanate structure is topologically similar to the wadeite and benitoite structures described above, in that it also features a silicate framework of alternating three-tetrahedra rings and isolated octahedra. Ten-coordinated Ba cations occupy channels in the silicate framework.

This material was synthesized as single crystals by Fursenko (1997), and it comes from the same sample that was ground by Finger et al. (1995) in their Rietveld powder diffraction study of the benitoite form of BaSi_4O_9 , as described above. Evidently, grinding transforms the barium germanate-type single crystals to the closely-related benitoite form, which is 4.2% less dense.

The wadeite structure ($m = 2$; $n = 6$).

Several high-pressure framework silicates have $n/m = 3$, in which tetrahedral rings alternate with silicate octahedra. The wadeite-type ($\text{K}_2\text{ZrSi}_3\text{O}_9$) structure, along with the benitoite-type and barium germanate-type structures (see below), feature a corner-linked framework of alternating three-tetrahedra rings and isolated octahedra. In wadeite, Si_3O_9 three-tetrahedra rings are cross-linked by Zr octahedra, forming a framework with hexagonal symmetry (space group $P6_3/m$; Fig. 13). Potassium occupies nine-coordinated cavities between adjacent three-member Si tetrahedral rings. Germanate isomorphs, including $\text{K}_2\text{GeSi}_3\text{O}_9$ (Reid et al. 1967), $\text{K}_2\text{Ge}_4\text{O}_9$ (Voellenkle and Wittmann 1971) and $(\text{LiNa})\text{Ge}_4\text{O}_9$ (Voellenkle et al. 1969), pointed the way for Kinomura et al. (1975), who observed the high-pressure $^{\text{VI}}\text{Si}$ analog, $\text{K}_2\text{Si}_4\text{O}_9$. Their polycrystalline sample was produced at 9 GPa and 1200°C .

In the silica-rich isomorph, $\text{K}_2^{\text{VI}}\text{Si}^{\text{IV}}\text{Si}_3\text{O}_9$, silicon occurs in all network-forming positions, in both four- and six-

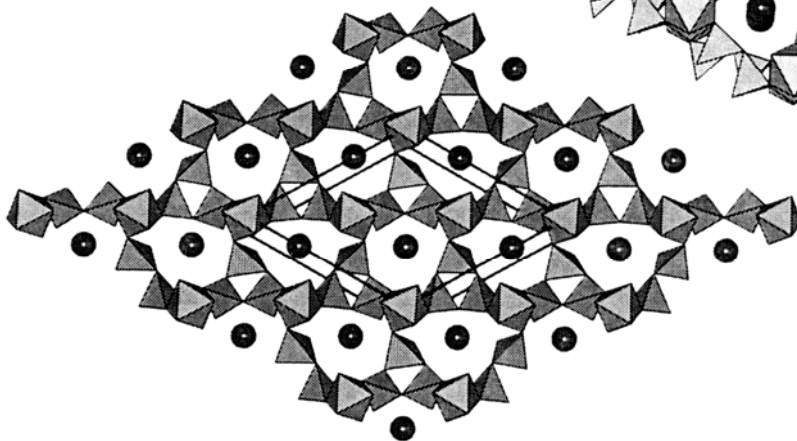
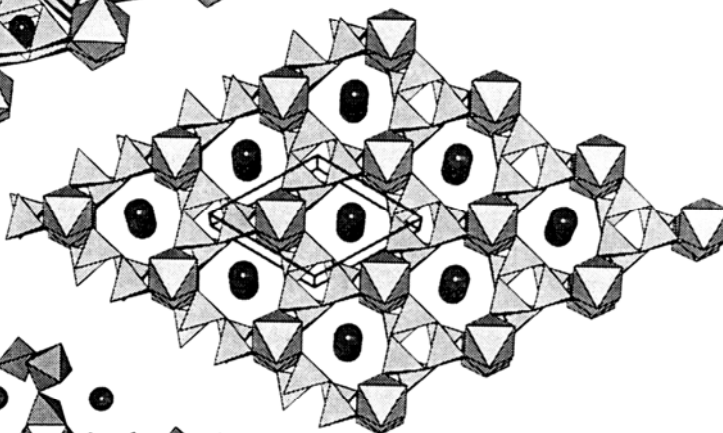
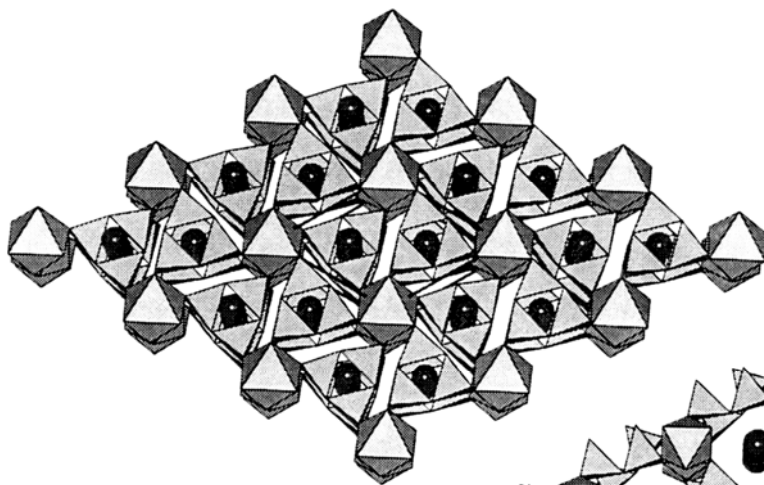


Figure 13. The wadeite-type crystal structure.

Figure 14. The benitoite-type crystal structure.

Figure 15. The barium germanate-type crystal structure.

This $P3$ barium germanate structure, the $P\bar{6}c2$ benitoite structure, and the trigonal $P321$ structure of BaGe_4O_9 (Smolin 1968) and SrGe_4O_9 (Nishi 1996) are strikingly similar in topology. All possess the distinctively layered corner-linked framework structure of alternating three-tetrahedra rings and isolated octahedra, with alkaline earth cations in large structural channels. Significant differences among these three structure types occur in the average values of interpolyhedral angles. In the barium germanate-type BaSi_4O_9 , average $^{\text{IV}}\text{Si-O-}^{\text{IV}}\text{Si}$ angles within the three-member rings are 128.1° and average $^{\text{IV}}\text{Si-O-}^{\text{VI}}\text{Si}$ angles between the rings and octahedra are 127.8° . Ten Ba-O bonds are within 3.2 \AA , with a mean Ba-O distance of 2.898 \AA . By contrast, in the benitoite form of BaSi_4O_9 , which is 4.2% less dense, average $^{\text{IV}}\text{Si-O-}^{\text{IV}}\text{Si}$ and $^{\text{IV}}\text{Si-O-}^{\text{VI}}\text{Si}$ angles are 133.6° and 136.1° , respectively. Only six Ba-O bonds are within 3.2 \AA (all at 2.743 \AA) and the mean Ba-O distance of 12-coordinated barium is 3.011 \AA . The lower density of the benitoite polymorph thus arises from the more open framework with larger Si-O-Si angles.

Comparisons of these structures with the $P321$ structure of SrGe_4O_9 (Nishi 1996) are instructive. The mean $^{\text{IV}}\text{Ge}-\text{O}-^{\text{IV}}\text{Ge}$ and $^{\text{IV}}\text{Ge}-\text{O}-^{\text{VI}}\text{Ge}$ angles are 122.1° and 118.6° , respectively—values significantly smaller than in the benitoite or barium germanate forms of BaSi_4O_9 . Thus, while comparisons between silicates and germanates must be made with caution, it is possible that the $P3$ structure might transform to a more tilted, and consequently denser, $P321$ form at higher pressure.

New sodium tetrasilicate structure ($m = 2; n = 6$). Fleet (1996) described the structure of a new sodium tetrasilicate, $\text{Na}_6^{\text{VI}}\text{Si}_3(^{\text{VI}}\text{Si}_9\text{O}_{27})$, which was synthesized at pressures between 6 and 9 GPa and temperatures from 1000° to 1500°C . The complex structure is monoclinic (space group $P2_1/n$), with 43 symmetrically distinct atoms (Fig. 16). This unusual framework silicate features nine-member tetrahedral rings that are cross-linked by isolated silicate octahedra in a layered arrangement. Because of the involute nature of the nine-member ring, the local coordination environment of both silicate octahedra and tetrahedra are quite similar to those in the wadeite, benitoite, and barium germanate structures described above.

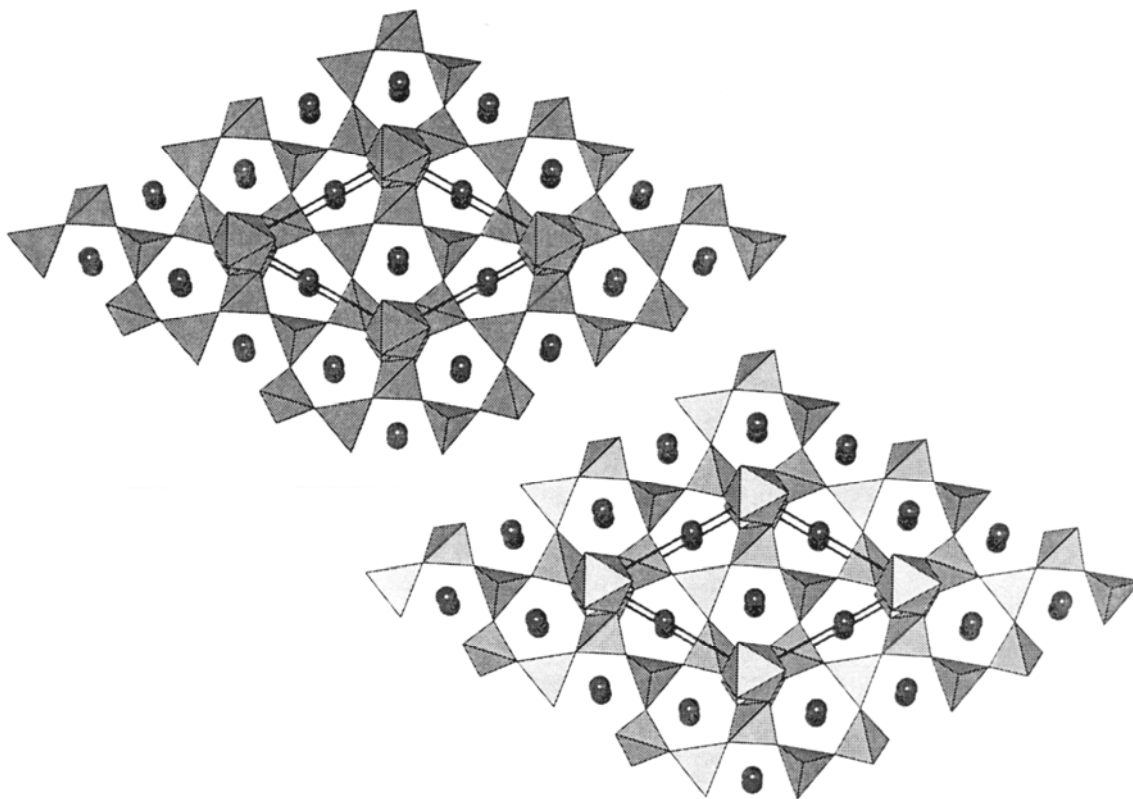


Figure 16. The crystal structure of a new sodium tetrasilicate.

Figure 17. The crystal structure a new sodium-calcium hexasilicate.

This structure underscores the prediction of Finger and Hazen (1991) that complex crystal chemistry is not restricted to low-pressure, low-density silicates. Fleet (1996) concludes, “even transition-zone pressures do not dominate the stereochemical requirements of the large cations in determining the structures of the alkali and alkaline-earth aluminosilicates.”

New sodium-calcium hexasilicate structure ($m = 1; n = 5$). The four framework structure types described above—wadeite, benitoite, barium germanate, and the new

sodium tetrasilicate—all have $n/m = 3$, resulting in fully-linked frameworks with tetrahedral rings. Every tetrahedron has two bridging T-O-T oxygen atoms, and two bridging T-O-^{VI}Si oxygen atoms. Structures with $n/m > 3$, however, cannot form fully-linked frameworks in this way.

Although many framework configurations with n/m might be imagined, only two such structures have been reported: the $n/m = 5$ structure reviewed in this section and the $n/m = 6$ structure described below. Gasparik et al. (1995) described the synthesis of a new sodium-calcium hexasilicate, $(\text{Na}_{1.8}\text{Ca}_{1.1})^{\text{VI}}\text{Si}^{\text{IV}}\text{Si}_5\text{O}_{14}$, which is a dominant phase in the system $\text{Na}_2\text{O}-\text{CaO}-5\text{SiO}_2$ at pressures between 8 and 14 GPa and temperatures between 950 and 2300°C. They proposed an ideal formula of $\text{Na}_2\text{CaSi}_6\text{O}_{14}$ for this phase. Single crystals suitable for X-ray study were obtained from synthesis experiments at 14 GPa and 1900°C. This trigonal framework silicate (space group $P321$) features unique tetrahedral layers of interconnected 12-member rings (Fig. 17). These layers are linked into a framework by isolated silicate octahedra.

A striking feature of the silicate layer is that two of every 14 oxygen atoms are nonbridging, being coordinated to one tetrahedrally-coordinated Si atom and three Na/Ca atoms. Nonbridging oxygen atoms are not observed in room-pressure framework silicates, and their presence in this structure and the sodium heptasilicate described below points to a rich and as yet little explored variety of stoichiometries, topologies, and crystal chemical behavior in high-pressure silicate frameworks.

New sodium heptasilicate structure ($m = 0.5$; $n = 3$): Fleet (1998) reported the intriguing new structure of sodium heptasilicate, $\text{Na}_8^{\text{VI}}\text{Si}^{\text{IV}}\text{Si}_6\text{O}_{18}$, with $n/m = 6$. Single crystals of this phase were synthesized at 9 GPa and 1000°C as part of their ongoing investigation of the $\text{Na}_2\text{O}-\text{SiO}_2$ system (Fleet and Henderson 1997). The trigonal structure (space group $R\bar{3}$) features six-member tetrahedral rings that are cross-linked by isolated silicate octahedra (Fig. 18). Each silicate octahedron is fully linked to six different tetrahedral rings, and the octahedral environment is thus similar to that of most other IV-VI framework silicates. The tetrahedra, on the other hand, are not fully linked; each tetrahedron is only linked to two other tetrahedra (within the six-membered ring) and one silicate octahedron, with one non-bridging oxygen on every tetrahedron. Two sodium atoms per formula unit are in distorted octahedral coordination, while the other six sodium atoms per formula unit are in eight-coordination.

Other structures with mixed ^{IV}Si and ^{VI}Si

The anhydrous phase B structure. Studies by Ringwood and Major (1967b) on hydrous magnesium silicates at high pressure revealed a complex material, designated phase B. This structure, although frequently observed in subsequent studies of magnesium silicates, remained unidentified until Finger et al (1989) obtained single crystals

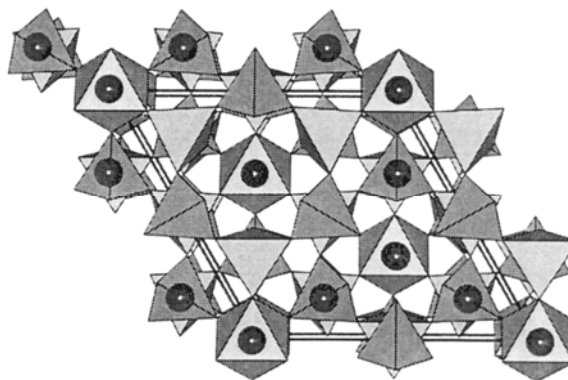


Figure 18. The crystal structure of a new sodium heptasilicate.

of a closely related anhydrous magnesium silicate, designated anhydrous phase B. The crystals of anhydrous phase B, identified as $\text{Mg}_{14}\text{Si}_5\text{O}_{24}$, facilitated the solution of both unknown structures.

Anhydrous phase B crystals were produced at the Mineral Physics Institute, State University of New York, Stony Brook, at 16.5 GPa and 2380°C. Routine solution by direct methods resulted in a structure that was subsequently found to be isostructural with $\text{Mg}_{14}\text{Ge}_5\text{O}_{24}$ (Von Dreele et al. 1970). The orthorhombic (space group $Pmcb$) structure is based on close packing of oxygen atoms and features a six-layer ($b = 14.2 \text{ \AA}$) stacking sequence. Layers of the first type contain Mg and Si in octahedral coordination, while the second type of layer contains magnesium octahedra and silicon tetrahedra in an olivine arrangement (Fig. 19). Layers are stacked 2-1-2-2-1-2. One surprising consequence of this sequence is that each silicon octahedron shares all twelve edges with adjacent magnesium octahedra in a distinctive cluster of 13 octahedra. Details of the structure are provided by Finger et al. (1991). Hazen et al. (1992) subsequently reported the structure of an Fe-bearing anhydrous phase B, $(\text{Mg}_{0.88}\text{Fe}_{0.12})_{14}\text{Si}_5\text{O}_{24}$, which displays a surprising degree of Fe ordering into one of the six symmetrically distinct Mg-Fe octahedral sites.

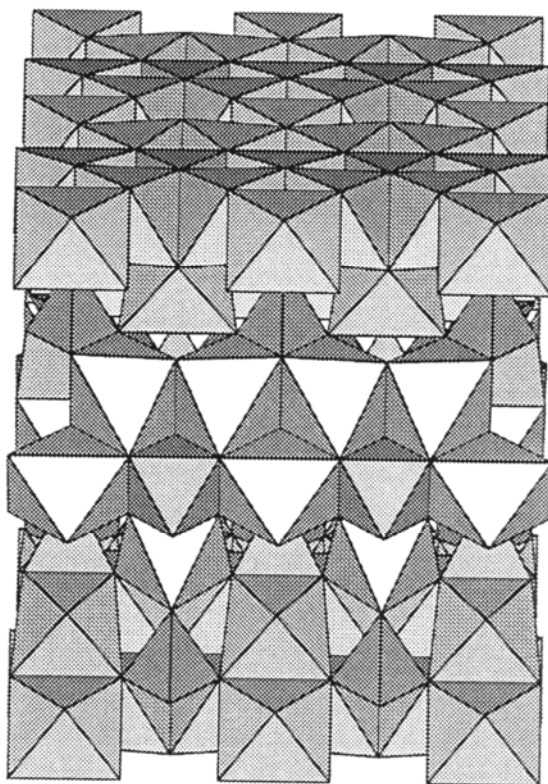


Figure 19. The crystal structure of anhydrous Phase B.

The phase B structure. The phase B structure was solved by Finger et al. (1989), who recognized its close similarity to anhydrous phase B and identified its composition as $\text{Mg}_{12}\text{Si}_4\text{O}_{19}(\text{OH})_2$. Single crystals synthesized at 12 GPa and 1200°C display similar cell parameters to anhydrous phase B (both structures have b and c axes of about 14.2 and 10.0 Å, respectively). The six-layer arrangement is similar in hydrous and anhydrous phase B, but the presence of OH causes periodic offsets in the layers and thus a reduction to monoclinic symmetry (space group $P2_1/c$; Fig. 20). Details of the structure are given by Finger et al. (1991).

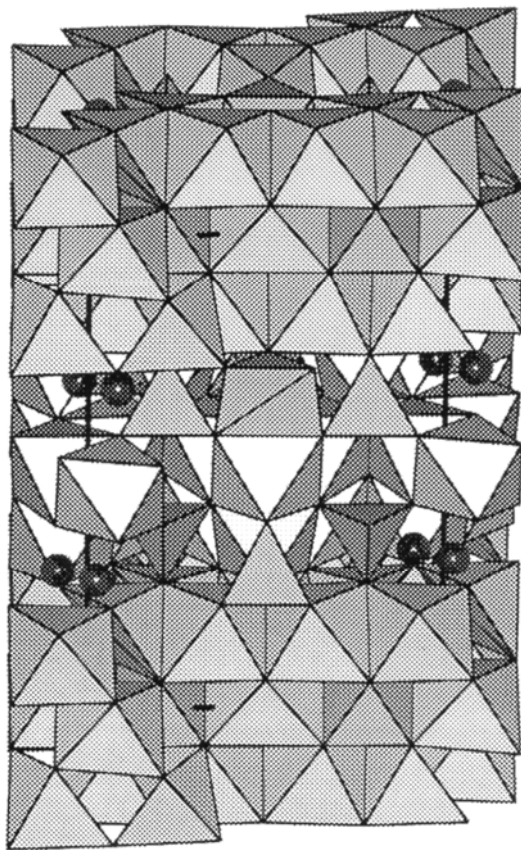


Figure 20. The crystal structure of Phase B.

The superhydrous phase B structure. A third magnesium silicate structure, $\text{Mg}_{10}\text{Si}_3\text{O}_{14}(\text{OH})_4$, was determined by Pacalo and Parise (1992) to be closely related to those of phase B and anhydrous phase B. They called this material superhydrous B, because it has twice the hydrogen content per formula unit as phase B. Single crystals were synthesized at 20 GPa and 1400°C by Pacalo and Gasparik (1990) from an oxide mix of $2\text{Mg}(\text{OH})_2$ and SiO_2 , equivalent to olivine + H_2O . The orthorhombic structure (space group $Pnmm$) is related to phase B by a shear of the olivine-like layers (Fig. 21). This structure, like the other two “B phases,” consists of a six-layer repeat parallel to b , and it also features the 12Mg-Si cluster of octahedra.

Hazen et al. (1997) described the isostructural superfluorous phase B, $\text{Mg}_{10}\text{Si}_3\text{O}_{14}\text{F}_4$, which was synthesized by Gasparik (1993) at 17.8 GPa and temperatures between 1450° and 1600°C. All dimensions and bond distances for the fluorous variant are within 1% of those of superhydrous phase B.

The pyroxene structure. Pyroxenes, among the most common constituents of igneous and metamorphic rocks, typically have compositions $A\text{SiO}_3$ where A may consist entirely of divalent Mg, Fe and Ca or may contain a mixture of cations with +1, +2 and +3 valences. Angel et al. (1988) described an unusual high-pressure synthetic pyroxene with composition $\text{Na}^{\text{VI}}(\text{Mg}_{0.5}\text{Si}_{0.5})^{\text{IV}}\text{Si}_2\text{O}_6$. Silicon and magnesium form an ordered edge-sharing octahedral chain in this structure.

High-pressure synthesis of other silica-rich biopyriboles (Finger et al. 1998) indicates that such a substitution scheme may occur in a wide range of pyroxene- and amphibole-like structures. Angel et al. (1988) note, however, that it is doubtful such

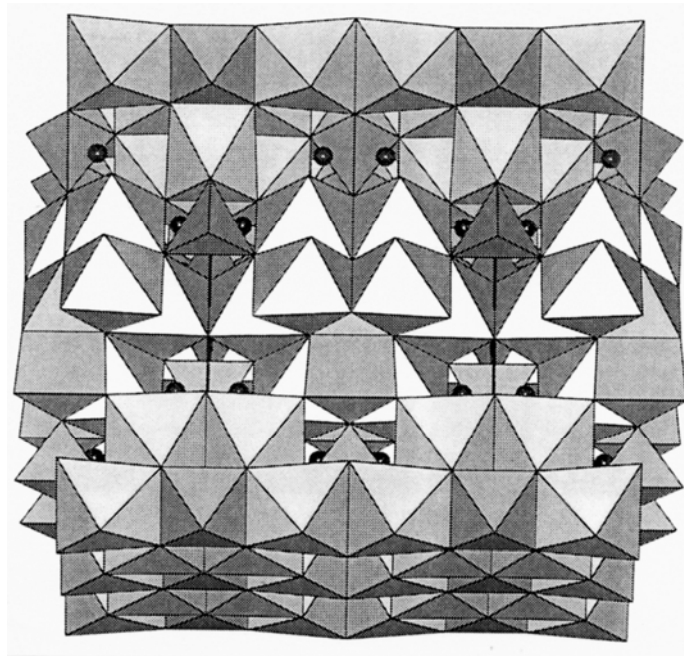


Figure 21. The crystal structure of superhydrous Phase B.

silica-rich biopyriboles play a significant role in the Earth's mantle, for their stability will be limited to silica-rich compositions with an excess of alkalis with respect to aluminum—a situation rarely encountered in nature.

The spinel structure. A discussion of structures with both ^{VI}Si and ^{IV}Si would not be complete with mention of silicate spinels, which have long been recognized as high-pressure variants of ferromagnesian orthosilicate, $(\text{Mg,Fe})_2\text{SiO}_4$. Most synthetic samples are observed to be close to fully ordered, with all silicon in tetrahedral coordination and (Mg,Fe) in octahedral coordination, but the possibility of some cation disorder, and hence some ^{VI}Si under mantle conditions, has long been recognized (Jackson et al. 1974, Liebermann et al. 1977). Samples rapidly quenched from high temperature and high pressure may be slightly disordered, with a few percent Si in octahedral coordination and a corresponding percent of Mg in tetrahedral coordination. Direct evidence for this behavior was inferred by Hazen et al. (1993) from unusually long T-O distances in a series of Mg-Fe silicate spinels synthesized at 20 GPa and 1400°C.

Predictions of spinel compressibilities (Liebermann et al. 1977, Hazen and Yang 1999) indicate that disordered silicate spinels should be significantly more compressible than ordered variants because of the relative stiffness of tetrahedral Si-O bonds. Thus, disordered silicate spinels with significant ^{VI}Si may occur in the Earth's lower mantle.

SYSTEMATICS OF ^{VI}Si STRUCTURES AND PREDICTIONS OF OTHER HIGH-PRESSURE PHASES

^{VI}Si -O bond distances and interpolyhedral linkages

Octahedral Si-O distances and interpolyhedral linkages for the ^{VI}Si structure types described above are summarized in Table 4. This table includes data for 18 structures at room conditions for which three-dimensional refinements are available. Data are not included in this table for the incomplete or internally inconsistent refinements of the pyrochlore-, potassium nickel fluoride-, and calcium ferrite-type ^{VI}Si structures, as well as for calcium chloride-type SiO_2 , which only occurs at high pressure. Also excluded are

Table 4. Octahedral Si-O distances (Å) and interpolyhedral linkages

Structure	Min Si-O	Max Si-O	Mean Si-O	Interpolyhedral linkages shared			Reference
				Corners	Edges	Faces	
SiO ₂	1.757	1.809	1.774	4 to ^{VI} Si 2 to 2 ^{VI} Si	2 to ^{VI} Si	-	Ross et al. (1990)
CaSiO ₃ (Pv)	1.784	1.784	1.784	6 to ^{VI} Si	-	-	Mao et al. (1989)
MgSiO ₃ (Pv)	1.779	1.801	1.792	6 to ^{VI} Si	-	-	Ross & Hazen (1990)
MgSiO ₃ (Ilm)	1.768	1.830	1.799	3 to ^{VI} Mg 3 to 2 ^{VI} Mg	3 to ^{VI} Si	1 to ^{VI} Mg	Horiuchi et al. (1982)
MgSi ₂ O ₄ (OH) ₂	1.805	1.805	1.805	-	3 to ^{VI} Si 6 to ^{VI} Mg	-	Yang et al. (1997)
AlSiO ₃ (OH)	1.740	2.066	1.814	6 to ^{VI} Al	1 to ^{VI} Si 2 to ^{VI} Al	-	Schmidt et al. (1998)
CaSi ₂ O ₅	1.709	1.862	1.798	2 to ^{VI} Si 4 to ^{IV} Si	-	-	Angel (1997)
Na ₂ Si ₃ O ₇	1.765	1.819	1.789	6 to ^{IV} Si	-	-	Fleet & Henderson (1995)
K ₂ Si ₄ O ₉	1.797	1.818	1.804	6 to ^{IV} Si	-	-	Swanson & Prewitt (1983)
BaSi ₄ O ₉	1.770	1.770	1.770	6 to ^{IV} Si	-	-	Finger et al. (1995)
BaSi ₄ O ₉	1.758	1.767	1.763	6 to ^{IV} Si	-	-	Hazen et al. (1999)
Na ₆ Si ₁₂ O ₂₇	1.754	1.821	1.781	6 to ^{IV} Si	-	-	Fleet (1996)
Na ₂ CaSi ₆ O ₁₄	1.789	1.789	1.789	6 to ^{IV} Si	-	-	Gasparik et al. (1995)
Na ₈ Si ₇ O ₁₈	1.816	1.816	1.816	6 to ^{IV} Si	-	-	Fleet (1998)
Anhy B	1.797	1.818	1.804	-	12 to ^{VI} Mg	-	Finger et al. (1989)
Phase B	1.787	1.897	1.813	-	12 to ^{VI} Mg	-	Finger et al. (1989)
Shy B	1.770	1.903	1.814	-	12 to ^{VI} Mg	-	Pacalo & Parise (1992)
Na-Pyroxene	1.782	1.826	1.811	6 to ^{IV} Si	2 to ^{VI} Mg	-	Angel et al. (1988)

the hollandite-, pyroxene-, garnet-, and spinel-type structures with disordered Al-Si or Mg-Si octahedra.

Of special interest is the variety of linkages between Si octahedra and other octahedra and tetrahedra. In stishovite, hollandite, and pyroxene a combination of edge and corner sharing is observed, but in the “phase B” structures each Si octahedron shares all 12 edges with adjacent Mg octahedra. In perovskite, pyrochlore, and the varied IV-VI framework silicates, the SiO₆ octahedra form part of a corner-linked framework, but additional cations in eight or greater coordination share edges and faces with the octahedra. Ilmenite presents yet a different topology, with unusual face sharing between Mg and Si octahedra, as well as corner and edge sharing.

In spite of the variety of polyhedral linkages, the size and shape of SiO₆ polyhedra are similar in all these compounds. Mean Si-O distances vary by only ±2% about the overall mean distance of 1.796 Å. Finger and Hazen (1991), similarly, found that polyhedral volumes vary by only about ±4% from an average value of approximately 7.6 Å³. Most Si octahedra are close to regular (i.e. distortion indices are small) relative to the range often observed for octahedra of divalent and trivalent cations. These trends are consistent with the observation of Robert Downs (pers. comm.) that SiO₆ groups, in all structures for which anisotropic thermal parameters have been determined, display rigid-body vibrational motion. Similar behavior is displayed by SiO₄ and AlO₄ tetrahedra in silicates (Downs et al. 1990). Stebbins and Kanzaki (1991) used the distinctive NMR

signature of these rigid groups to determine structural characteristics of a number of high-pressure silicates in the system Ca-Si-O, and ^{29}Si NMR continues to provide a valuable structural probe for silicon coordination in small or poorly crystallized samples.

Other possible $^{\text{VI}}\text{Si}$ structures

The structure types detailed above form an eclectic group of silicate compositions and topologies. As demonstrated by Finger and Hazen (1991) and Hazen et al. (1996), however, systematic relations among the structures can be used to predict other possible $^{\text{VI}}\text{Si}$ phases. Three of these trends systematize groups of structurally-related phases:

1. The rutile-, calcium chloride-, hollandite-, and calcium ferrite-type structures, as well as the new “phase egg” structure, form from edge-sharing chains of silicate octahedra.
2. Three homologous structures in the system Mg-Si-O-H, including phase B, anhydrous phase B, and superhydrous phase B, feature edge-sharing clusters of twelve magnesium-oxygen octahedra surrounding a silicate octahedron.
3. Nine different alkali and alkaline earth framework silicate structures exhibit corner-linked arrays of silicate octahedra and tetrahedra.

The other three criteria are based on similarities between high-pressure silicates and room-pressure isomorphs.

4. Most of these high-pressure $^{\text{VI}}\text{Si}$ structures are isomorphs of room-pressure germanates with octahedrally-coordinated Ge.
5. Most of these high-pressure silicates are isomorphs of room-pressure oxides with trivalent or tetravalent transition metals (Ti, Mn, or Fe) in octahedral coordination.
6. High-pressure forms of ilmenite, pyroxene, and garnet are isomorphs of room-pressure aluminates, related to the high-pressure silicates by the substitution $2(^{\text{VI}}\text{Al}) \Rightarrow ^{\text{VI}}(\text{Mg} + \text{Si})$.

In spite of the limited number of known $^{\text{VI}}\text{Si}$ structures, these six trends point to the probable existence of many more such phases. In the following section we examine each of these criteria to predict other potential $^{\text{VI}}\text{Si}$ phases.

High-pressure silicates with $^{\text{VI}}\text{Si}$ edge-sharing chains. The rutile-type, cesium chloride-type, hollandite-type, calcium ferrite-type, and “phase egg” structures—five of the ten known high-pressure structures with all silicon in octahedral coordination—feature edge-sharing octahedral chains that are linked to adjacent strips by corner sharing, as systematized by Wadsley (1964), Bursill and Hyde (1972), and Bursill (1979). Rutile has single chains, leading to square channels that are 1 octahedron \times 1 octahedron wide. The hydrous aluminosilicate, “phase egg,” features a closely-related edge-sharing $2\text{Al}-2\text{Si}$ octahedral chain with offsets every fourth octahedron, resulting in channels that are effectively 1 \times 1.5 octahedra wide. Hollandite and calcium ferrite have double chains, yielding larger channels.

Many similar octahedral chain structures, such as ramsdellite (1 \times 2) and psilomelane (2 \times 3), are also known (Fig. 22) and each of these could provide a topology suitable for silicon in six coordination. Bursill (1979) explored a wide variety of hypothetical MX_2 structures created by juxtaposition of single-, double-, and triple-width octahedral chains. Both ordered and disordered phases with mixtures of rutile, ramsdellite, hollandite and psilomelane channels were examined. A surprising feature of these structures is that all could be constructed from the simple stoichiometry, SiO_2 . In fact, most of the compounds in this group of structures display coupled substitution of a channel-filling alkali or alkaline-earth cation plus Al for the octahedral cation. Only the

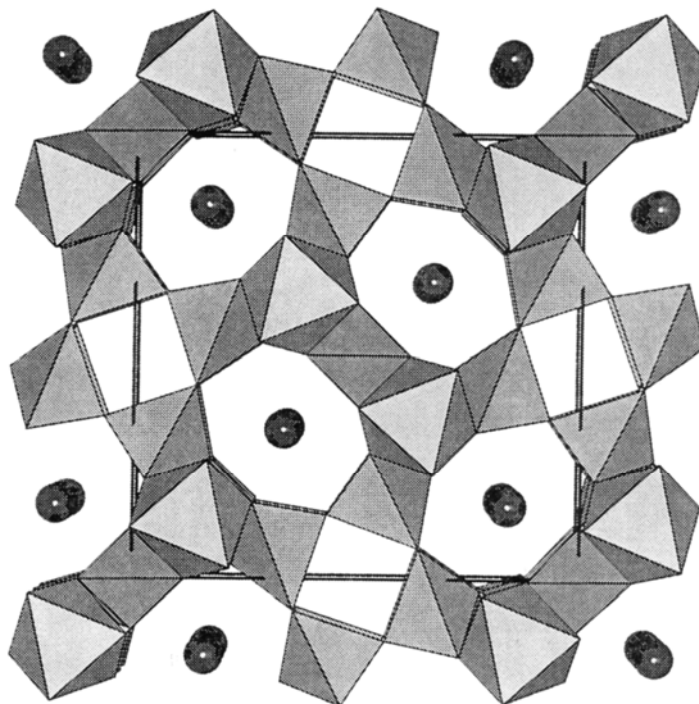


Figure 22. The crystal structure of $\text{Ca}_4\text{Ge}_5\text{O}_{16}$.

structures of rutile (TiO_2), iridium selenide (IrSe_2) and ramsdellite ($(-\text{MnO}_2)$) are known without additional cations in the channels.

Note that the systematic treatments of Bursill (1979) did not extend to octahedral strips with offsets, as observed in the novel “phase egg” structure. Offset octahedral strips, especially in conjunction with ordered arrangements of $^{\text{VI}}\text{Si}$ and trivalent cations, might significantly expand the topological variety of these phases.

Bursill (1979) also considered the possible role of trivalent cations in octahedral strip structures. He extended his discussion to a number of more-complex structures that combine the MX_2 forms described above with $\beta\text{-Ga}_2\text{O}_3$ topology, which is based on the same type of double edge-shared chains as found in hollandite. In $\beta\text{-Ga}_2\text{O}_3$ the double octahedral strips are cross-linked by GaO_4 tetrahedra. A range of gallium titanates, such as Ga_4TiO_8 , $\text{Ga}_4\text{Ti}_7\text{O}_{20}$ and $\text{Ga}_4\text{Ti}_{21}\text{O}_{48}$ (all members of the homologous series $\text{Ga}_4\text{Ti}_{m-4}\text{O}_{2m-2}$ that couple rutile and ($\gamma\text{-Ga}_2\text{O}_3$ units) are illustrated, as are ternary Ba-Ga-Ti oxides that unite components of rutile, hollandite and ($\gamma\text{-Ga}_2\text{O}_3$. All of these phases could accommodate $^{\text{VI}}\text{Si}$ and trivalent 4- and 6-coordinated cations at high pressure.

Systematics of phase B and other high-pressure hydrous magnesium silicates. The three closely related structures of phase B, anhydrous phase B, and superhydrous phase B are all based on alternate stacking of forsterite-type layers (with $^{\text{VI}}\text{Mg}$ and $^{\text{IV}}\text{Si}$) and octahedral layers (with $^{\text{VI}}\text{Mg}$ and $^{\text{VI}}\text{Si}$). Finger and Prewitt (1989) documented the close structural relations among a number of hydrous and anhydrous magnesium silicates and used those systematics to propose several as yet unobserved structures, including high-pressure hydrous phases with octahedral silicon. They recognized that several known phases, including chondrodite, humite, forsterite, phase B, and anhydrous phase B, are members of a large group of homologous magnesium silicates that can be represented by the general formula:

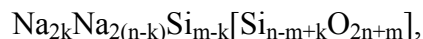


where $\text{mod}(n,2)$ is the remainder when n is divided by 2. Finger and Prewitt (1989) examined cases where $n = 1, 2, 3, 4, \infty$ and $m = 1, 2, \infty$. Structures with octahedral silicon result for all cases where m is not infinity.

High-pressure framework silicates. Hazen et al. (1996) systematized high-pressure alkali and alkaline-earth framework silicates with $^{\text{VI}}\text{Si}$ under the general formula:



where $0 \leq x \leq 2$ (total alkali and alkaline earth cations are thus normalized to +4). Fleet (1998) proposed an alternative structural formula for a homologous series of high-pressure sodium silicates:



with $k < m < n$ and $(n - m + k) \geq (3/2)(m - k)$.

At least three additional framework structures, known as room-pressure germanates, point to the likely existence of additional high-pressure silicate examples of such IV-VI frameworks. Alkali tetragermanates, $\text{A}_2\text{Ge}_4\text{O}_9$, adopt a trigonal (space group $P\bar{3}c1$) structure with three-member tetrahedral rings corner-linked to isolated octahedra. This structure is topologically similar to the wadeite structure, but the rings are more tilted in the tetragermanate structure (Choisnet et al. 1973). The trigonal strontium tetragermanate structure, SrGe_4O_9 (space group $P321$) as described by Nishi (1996), also features three-member tetrahedral rings and bears a close relationship to the wadeite, barium germanate, and benitoite structures (Hazen et al. 1999). A third example of special interest is the distinctive structure of calcium germanate, $\text{Ca}_2^{\text{VI}}\text{Ge}_2^{\text{IV}}\text{Ge}_5\text{O}_{16}$ (Nevskii et al. 1979b), which incorporates both four-member tetrahedral rings and isolated SiO_4 tetrahedra, corner-linked to isolated SiO_6 octahedra (Fig. 23).

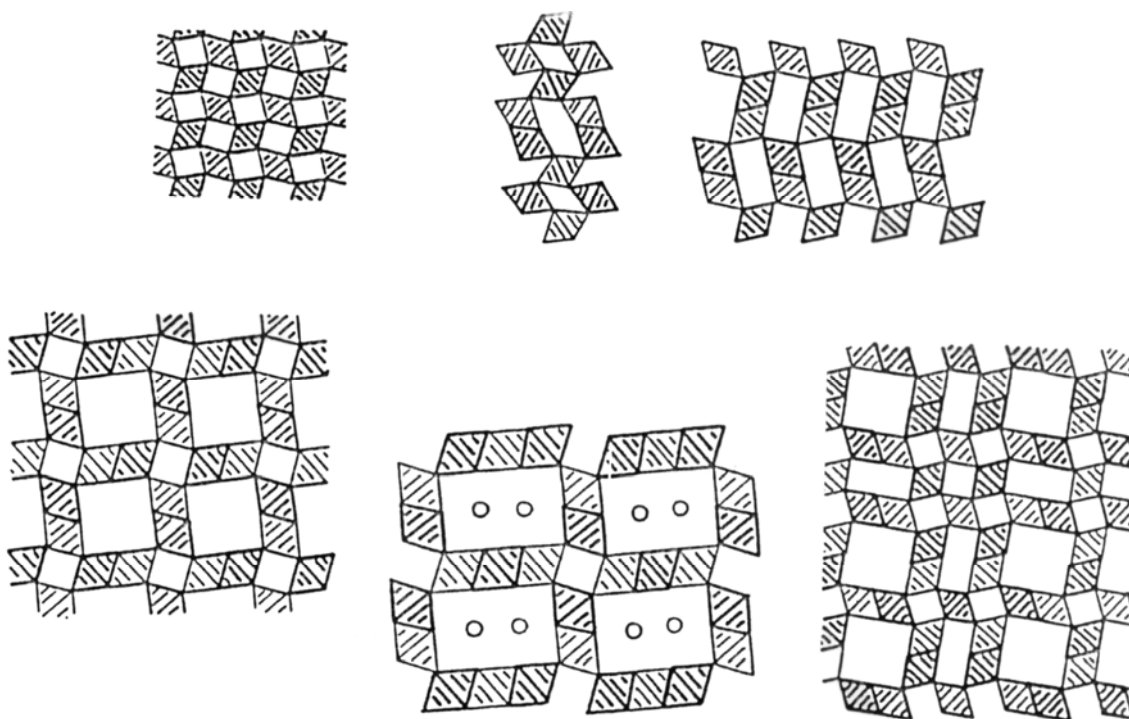


Figure 23. A comparison of several silicates with edge-linked octahedral chains.

Silicates based on substitution of ^{VI}Si for ^{VI}Ge . Most of the two dozen known ^{VI}Si high-pressure structure types were first synthesized as germanates at lower pressures. Room-pressure germanate crystal chemistry, therefore, may serve as a guide for high-pressure silicates.

In predicting high-pressure silicate isomorphs of these known room-pressure germanates, it is important to take into account the relative compressibilities of the different cation polyhedra. Large monovalent and divalent cations, such as Na, K and Ca, form polyhedra that are much more compressible than tetravalent Ge or Si. Since the stability of many structures depends critically on the cation radius ratio (Pauling 1960), it may be appropriate to substitute a smaller divalent cation when attempting to synthesize high-pressure forms. Thus, a high-pressure isomorph of CaGe_2O_5 might be MgSi_2O_5 while CaSi_2O_5 might be unstable.

^{VI}Si silicate isomorphs of transition-metal oxides. Most known high-pressure silicates with all silicon as ^{VI}Si adopt the structures of room-pressure oxides with Ti, Mn, or Fe^{3+} . Structures of other binary oxides with octahedral titanium, manganese, or ferric iron thus represent possible topologies for high-pressure minerals.

Numerous other octahedral transition-metal structures could be considered, as well. For example, there are many complex Ti, Mn, and Fe^{3+} borates (e.g. Moore and Araki 1974), based on frameworks of BO_3 triangles and columns and sheets of transition-metal octahedra. The K_2NiF_4 structure, adopted by Ca_2SiO_4 at high pressure, is just one of a wide variety of layered perovskite-related phases (Subramanian et al. 1988, Hazen 1990). A perplexing array of natural and synthetic tantalates, niobates, and uranium compounds incorporate Ti, Mn, Fe^{3+} , and other transition-metal octahedra with larger irregular cation polyhedra. As the search for high-pressure ^{VI}Si compounds extends to chemical systems beyond common rock-forming elements, new structures will undoubtedly be found among isomorphs of these known phases.

Silicates based on the substitution $^{VI}(\text{Si} + \text{Mg})$ for 2^{VI}Al . High-pressure ilmenite, garnet, and pyroxene forms of magnesium-bearing silicates are all related to room-pressure phases by the substitution of octahedral Mg and Si for a pair of Al cations. Similar substitutions might occur in several other common rock-forming minerals at high pressures. Note that this substitution scheme will not work for many common aluminum-bearing minerals with mixed four- and six-coordinated aluminum. The substitution in muscovite, $\text{K}^{VI}\text{Al}_2^{IV}(\text{AlSi}_3)\text{O}_{10}(\text{OH})_2$, for example, would yield the magnesian mica celadonite, $\text{K}^{VI}(\text{MgAl})^{IV}\text{Si}_4\text{O}_{10}(\text{OH})_2$, in which all Si is tetrahedrally coordinated. Octahedral Al, thus, must constitute more than two thirds of all aluminum atoms to produce an ^{VI}Si phase by the substitution $2\text{Al} \Rightarrow (\text{Mg} + \text{Si})$.

Summary of predicted structures

Table 5 lists examples of predicted ^{VI}Si compounds, based on the six structural and compositional criteria outlined above.

Several predicted compounds in Table 5 fulfill more than one of the six criteria. These structures thus seem particularly promising for further study. Of special interest to earth scientists are Fe_2SiO_5 with the pseudobrookite structure and $\text{Mg}_{10}\text{Si}_3\text{O}_{16}$ with the aerugite structure. These phases, or their isomorphs with other cations replacing Ca, Mg and Fe, might be represented in the Earth's mantle. Also worthy of further study are the proposed hydrous phases, $\text{MgSiO}_2(\text{OH})$ and $\text{MgSi}(\text{OH})_6$, which are isomorphs of diaspore and stottite, respectively. Such hydrogen-rich phases would be expected to occur only locally in the Earth's deep interior, but their presence, integrated over the Earth's volume, could represent a major repository of water.

Table 5. Examples of predicted ^{VI}Si compounds, based on six criteria*

Predicted composition	Structure type	Criteria*						Reference
		(1)	(2)	(3)	(4)	(5)	(6)	
KAlSi ₂ O ₆	IrSe ₂	X						Bursill (1979)
SiO ₂	Ramsdellite	X				X		Bursill (1979)
Ga ₄ SiO ₈	Ga ₄ TiO ₈	X				X		Bursill (1979)
Ga ₄ Si ₇ O ₂₀	Ga ₄ Ti ₇ O ₂₀	X				X		Bursill (1979)
(MgSi)O ₂ (OH) ₂	Diaspore	X					X	Smyth & Bish (1988)
Mg ₇ Si ₂ O ₁₀ (OH) ₂	B-type		X					Finger & Prewitt (1989)
Mg ₁₀ Si ₃ O ₁₆	Aerugite	X		X				Fleet & Barbier (1989)
K ₂ Si ₄ O ₉	K ₂ Ge ₄ O ₉			X	X			Choisnet et al. (1973)
SrSi ₄ O ₉	SrGe ₄ O ₉			X	X			Nishi (1996)
Ca ₂ Si ₇ O ₁₆	Ca ₂ Ge ₇ O ₁₆			X	X			Nevskii et al. (1980)
Fe ₄ Si ₂ O ₉	Fe ₄ Ge ₂ O ₉				X			Modaressi et al. (1984)
Fe ₈ Si ₃ O ₁₈	Fe ₈ Ge ₃ O ₁₈				X			Agafonov et al. (1986)
Fe ₂ SiO ₅	Pseudobrookite			X		X		Smyth & Bish (1988)
(MgSi)(OH) ₆	gibbsite, stottite			X		X		Ross et al. (1988)
(MgSi)SiO ₅	kyanite					X		Smyth & Bish (1988)

*Criteria are: (1) structures with edge-sharing octahedral strips; (2) Phase B-related structures; (3) IV-VI framework silicates; (4) germanate isomorphs; (5) isomorphs of 3+ and 4+ transition metal oxides; (6) structures related by the substitution 2 Al ⇒ Mg + Si.

In spite of these predictions, many yet to be determined high-pressure silicates are likely to have structures that fall outside the six criteria. The past decade has seen the discovery of new, unexpected dense silicates structures with offset edge-sharing octahedral strips (“phase egg”), dioctahedral silicate layers (phase D), and IV-VI framework structures with non-bridging oxygen atoms (Na-Ca hexasilicate and Na-heptasilicate). These new topologies occur in ternary and quaternary oxide systems, which are only just beginning to receive systematic attention at mantle conditions.

Most common rock-forming cations, including Na, Mg, Fe, Ca, Mn, Al, Ti, and Si, are small enough to fit into the tetrahedral or octahedral interstices of a close-packed oxygen net. However, the presence of many other cations, including H, B, K, Rb, Pb, rare earths and U, could disrupt the close-packed array and lead to other, as yet unrecognized, structure types. The gallium silicates in Table 5 are just two of the dozens of possible new ^{VI}Si structures likely to be observed as high-pressure investigations extend beyond the traditional rock-forming elements. These structures are not likely to play a significant role in mantle mineralogy, but they will provide a more complete understanding of the crystal chemistry of octahedral silicon.

CONCLUDING REMARKS

Finger and Hazen (1991) concluded their review of dense silicates by questioning whether the Earth’s deep interior is mineralogically simple. Are only a few structure types dominant, or is there an unrecognized complexity in the crystal chemistry of octahedral silicon? Volume constraints imposed by high pressure would seem to favor structures with approximately close-packed O atoms, thus reducing the number of

possible cation configurations as well. Nevertheless, within these restrictions there exist opportunities for considerable structural diversity based on three factors—reversible phase transitions, cation positional ordering, and modularity, particularly based on different close-packed layer-stacking sequences. This potential diversity is only hinted at by the known phases.

Several of the known high-pressure structure types, including perovskite, K_2NiF_4 , hollandite, titanite, and pyrochlore, can adopt numerous structural variants based on slight changes in lattice distortions and cation distribution. The perovskite structure, in particular, can undergo dozens of phase transitions based on octahedral tilting, cation ordering, cation displacements and anion defects (Megaw 1973, Hazen 1988). We must study proposed mantle phases at the appropriate conditions of pressure and temperature to document the equilibrium structural variations.

Close packing of oxygen atoms also leads to modular structures, with certain features (e.g. edge-sharing octahedral chains of rutile; the double chains of hollandite; the corner-sharing octahedral sheets of perovskite; the face-sharing topology of ilmenite) that can link together in many ways to form ordered superstructures of great complexity. Such complexity was recognized by Wadsley (1964) and Bursill (1979) in their descriptions of modular rutile-hollandite- β - Ga_2O_3 structures, and it is realized in the homologous series including phase B, anhydrous phase B, and superhydrous phase B. Phase B, for example, is based on oxygen close packing, yet it has 40 independent atoms in its asymmetric unit to yield one of the most complex ternary silicates yet described. Variations on the phase-B structure could be based on changing the relative number and position of the two different structural layers, by introducing other types of layers, or by staggering layers to produce clino- and ortho-type structures, as observed in other close-packed systems, for example, the biopyriboles as described by Thompson (1978) and Smith (1982). The structure could be further complicated by element ordering among the 17 different cation sites as Al, Fe, Ti, Mn, and other elements enter the structure in a natural environment.

Only two dozen high-pressure structure types with octahedrally-coordinated silicon have been documented, yet clear trends are beginning to emerge from the scattered data on diverse structures and compositions. It is now evident that, while silicate perovskite may be the predominant phase in the Earth's lower mantle, many other dense silicate structures incorporate elements such as Na, Ba, Ca and Al. Subduction of compositionally-varied crustal material deep into the mantle points to a rich, and as yet poorly understood, mineralogical diversity in the Earth's interior. The Earth's transition zone will display a richly varied mineralogy of mixed ^{VI}Si and ^{IV}Si silicates, including IV-VI framework structures of remarkable beauty and complexity. The lower mantle may also incorporate a previously unsuspected diversity of dense ^{VI}Si phases, including hydrous minerals that could play a significant role in the global water cycle. A detailed understanding of the mantle must await studies of these fascinating phases at temperatures and pressures appropriate to the Earth's dynamic interior.

REFERENCES

- Agafonov V, Kahn A, Michel D, Perez-y-Jorba M (1986) Structural investigation of a new iron germanate $Fe_8Ge_3O_{18}$. *J Solid State Chem* 62:397-401
- Akimoto S, Syono Y (1972) High-pressure transformations in $MnSiO_3$. *Am Mineral* 57:76-84
- Anderson DL (1976) The 650 km mantle discontinuity. *Geophys Res Lett* 3:347-349
- Angel RJ (1997) Transformation of fivefold-coordinated silicon to octahedral silicon in calcium silicate, $CaSi_2O_5$. *Am Mineral* 82:836-839
- Angel RJ, Gasparik T, Ross NL, Finger CT, Prewitt CT, Hazen RM (1988) A silica-rich sodium pyroxene phase with six-coordinated silicon. *Nature* 335:156-158

- Angel RJ, Finger LW, Hazen RM, Kanzaki M, Weidner DJ, Liebermann RC, Veblen DR (1989) Structure and twinning of single-crystal MgSiO₃ garnet synthesized at 17 GPa and 1800°C. *Am Mineral* 74:509-512
- Angel RJ, Ross NL, Seifert F, Fliervoet TF (1996) Structural characterization of a pentacoordinate silicon in a calcium silicate. *Nature* 384:441-444
- Baur WH, Khan AA (1971) Rutile-type compounds. IV. SiO₂, GeO₂ and a comparison with other rutile-type structures. *Acta Crystallogr B* 27:2133-2138
- Birch F (1952) Elasticity and constitution of the Earth's interior. *J Geophys Res* 57:227-286
- Bissert G, Liebau F (1970) Die Kristallstruktur von monoklinem Siliziumphosphat SiP₂O₇: eine Phase mit [SiO₆]-oktaedern. *Acta Cryst B* 26:233-240
- Bursill LA (1979) Structural relationships between α -gallia, rutile, hollandite, psilomelane, ramsdellite and gallium titanate type structures. *Acta Crystallogr B* 35:530-538
- Bursill LA, Hyde BG (1972) Rotation faults in crystals. *Nature Phys Sci* 240:122-124
- Chao ECT, Fahey JJ, Littler J, Milton DJ (1962) Stishovite, SiO₂, a very high pressure mineral from Meteor Crater, Arizona. *J Geophys Res* 67:419-421
- Choisnet J, Deschanvres A, Raveau B (1973) Evolution structurale de nouveaux germanates et silicates de type wadeite et de structure apparentée. *J Solid State Chem* 7:408-417
- Downs RT, Gibbs GV, Boisen MB Jr (1990) A study of the mean-square displacement amplitudes of Si, Al, and O atoms in rigid framework structures: evidence for rigid bonds, order, twinning, and stacking faults. *Am Mineral* 75:1253-1262
- Downs RT, Hazen RM, Finger LW, Gasparik T (1995) Crystal chemistry of lead aluminosilicate hollandite: A new high-pressure synthetic phase with octahedral Si. *Am Mineral* 80:937-940
- Durif A, Averbuch-Pouchot MT, Guitel JC (1976) Structure cristalline de (NH₄)₂SiP₄O₁₃: un nouvel exemple de silicium hexacoordine. *Acta Crystallogr B* 32:2957-2960
- Edge RA, Taylor HFW (1971) Crystal structure of thaumasite, [Ca₃Si(OH)₆12H₂O](SO₄)(CO₃). *Acta Crystallogr B* 27:594-601
- Effenberger H, Kirfel A, Will G, Zobetz E (1983) A further refinement of the crystal structure of thaumasite, Ca₃Si(OH)₆CO₃SO₄12H₂O. *Neues Jahrb Mineral Mh* 2:60-68
- Eggleton RA, Boland JN, Ringwood AE (1978) High-pressure synthesis of a new aluminum silicate: Al₅Si₅O₁₇(OH). *Geochem J* 12:191-194
- Fei Y, Saxena SK, Navrotsky A (1990) Internally consistent thermodynamic data and equilibrium phase relations for compounds in the system MgO-SiO₂ at high pressure and high temperature. *J Geophys Res* 95:6915-6928
- Fei Y, Wang Y, Finger LW (1996) Maximum solubility of FeO in (Mg,Fe)SiO₃-perovskite as a function of temperature at 26 GPa: Implication for FeO content in the lower mantle. *J Geophys Res* 101:11525-11530
- Finger LW, Hazen RM (1991) Crystal chemistry of six-coordinated silicon: a key to understanding the Earth's deep interior. *Acta Crystallogr B* 47:561-580
- Finger LW, Prewitt CT (1989) Predicted compositions for high-density hydrous magnesium silicates. *J Geophys Res Lett* 16:1395-1397
- Finger LW, Ko J, Hazen RM, Gasparik T, Hemley RJ, Prewitt CT, Weidner DJ (1989) Crystal chemistry of phase B and an anhydrous analogue: implications for water storage in the upper mantle. *Nature* 341:140-142
- Finger LW, Hazen RM, Prewitt CT (1991) Crystal structures of Mg₁₂Si₄O₁₉(OH)₂ (phase B) and Mg₁₄Si₅O₂₄ (phase AnhB). *Am Mineral* 76:1-7
- Finger LW, Hazen RM, Fursenko BA (1995) Refinement of the crystal structure of BaSi₄O₉ in the benitoite form. *J Phys Chem Solids* 56:1389-1393
- Finger LW, Yang H, Konzett J, Fei Y (1998) The crystal structure of a new clinopyroxene, a high-pressure potassium phase. *EOS Trans Am Geophys Union* 79(17), Spring Meeting Suppl, p S161
- Fleet ME (1996) Sodium tetrasilicate: a complex high-pressure framework silicate (Na₆Si₃[Si₉O₂₇]). *Am Mineral* 81:1105-1110
- Fleet ME (1998) Sodium heptasilicate: A high-pressure silicate with six-membered rings of tetrahedra interconnected by SiO₆ octahedra: (Na₈Si[Si₆O₁₈]). *Am Mineral* 83:618-624
- Fleet ME, Barbier J (1989) The structure of aerugite (Ni_{8.5}As₃O₁₆) and interrelated arsenate and germanate structural series. *Acta Crystallogr B* 45:201-205
- Fleet ME, Henderson GS (1995) Sodium trisilicate: a new high-pressure silicate structure (Na₂Si[Si₂O₇]). *Phys Chem Minerals* 22:383-386
- Fleet ME, Henderson GS (1997) Structure-composition relations and Raman spectroscopy of high-pressure sodium silicates. *Phys Chem Minerals* 24:345-355
- Fujino K, Momoi H, Sawamoto H, Kumazawa M (1986) Crystal structure and chemistry of MnSiO₃ tetragonal garnet. *Am Mineral* 71:781-785

- Fursenko BA (1997) New high-pressure silicon-bearing phases in hexad coordination. *Trans Russian Acad Sci Earth Sci* 353:227-229
- Gasparik T (1989) Transformations of enstatite-diopside-jadeite pyroxenes to garnet. *Contrib Mineral Petrol* 102:389-405
- Gasparik T (1990) Phase relations in the transition zone. *J Geophys Res* 95:15751-15769
- Gasparik T (1993) The role of volatiles in the transition zone. *J Geophys Res* 98:4287-4299
- Gasparik T, Parise JB, Eiben BA, Hriljac JA (1995) Stability and structure of a new high-pressure silicate, $\text{Na}_{1.8}\text{Ca}_{1.1}\text{Si}_6\text{O}_{14}$. *Am Mineral* 80:1269-1276
- Gillet P, Chen M, Dubrovinsky L, El Goresy A (2000) Natural $\text{NaAlSi}_3\text{O}_8$ -hollandite in the shocked Sixiangkou meteorite. *Science* 287:1633-1636
- Glazer AM (1972) The classification of tilted octahedra in perovskites. *Acta Crystallogr B* 28:3384-3392
- Haggerty SE, Sautter V (1990) Ultradeep (greater than 300 kilometers), ultramafic upper mantle xenoliths. *Science* 248:993-996
- Hazen RM (1988) Perovskites. *Sci Amer* June 1988:74-81
- Hazen RM (1990) Crystal structures of high-temperature superconductors. *In* *Physical Properties of High Temperature Superconductors II*, Ginsberg DM (ed) p 121-198. Singapore: World Scientific
- Hazen RM (1993) *The New Alchemists*. New York: Times Books
- Hazen RM, Finger LW (1978) Crystal chemistry of silicon-oxygen bonds at high pressure: implications for the Earth's mantle mineralogy. *Science* 201:1122-1123
- Hazen RM, Yang H (1999) Effects of cation substitution and order-disorder on P-V-T equations of state of cubic spinels. *Am Mineral* 84:1956-1960
- Hazen RM, Finger LW, Ko J (1992) Crystal chemistry of Fe-bearing anhydrous phase B: Implications for transition zone mineralogy. *Am Mineral* 77:217-220
- Hazen RM, Downs RT, Finger LW, Ko J (1993) Crystal chemistry of ferromagnesian silicate spinels: Evidence for Mg-Si disorder. *Am Mineral* 78:1320-1323
- Hazen RM, Downs RT, Conrad PG, Finger LW, Gasparik T (1994a) Comparative compressibilities of majorite-type garnets. *Phys Chem Minerals* 21:344-349
- Hazen RM, Downs RT, Finger LW, Conrad PG, Gasparik T (1994b) Crystal chemistry of Ca-bearing majorite. *Am Mineral* 79:581-584
- Hazen RM, Downs RT, Finger LW (1996) High-pressure framework silicates. *Science* 272:1769-1771
- Hazen RM, Yang Y, Prewitt CT, Gasparik T (1997) Crystal chemistry of superfluorous phase B ($\text{Mg}_{10}\text{Si}_3\text{O}_{14}\text{F}_4$): Implications for the role of fluorine in the mantle. *Am Mineral* 82:647-650
- Hazen RM, Yang H, Finger LW, Fursenko BA (1999) Crystal chemistry of BaSi_4O_9 in the trigonal (P3) barium tetragermanate structure. *Am Mineral* 84:987-989
- Heinemann S, Sharp TG, Seifert F, Rubie DC (1997) The cubic-tetragonal phase transition in the system majorite ($\text{Mg}_4\text{Si}_4\text{O}_{12}$)–pyrope ($\text{Mg}_3\text{Al}_2\text{Si}_3\text{O}_{12}$), and garnet symmetry in the Earth's transition zone. *Phys Chem Minerals* 24:206-221
- Hemley RJ, Cohen RE (1992) Silicate perovskite. *Ann Rev Earth Planet Sci* 20:553-600
- Hemley RJ, Prewitt CT, Kingma KJ (1994) High-pressure behavior of silica. *Rev Mineral* 29:41-81
- Hesse KF (1979) Refinement of the crystal structure of silicon diphosphate, SiP_2O_7 AIV—a phase with six-coordinated silicon. *Acta Crystallogr B* 35:724-725
- Hill RJ, Newton MD, Gibbs GV (1983) A crystal chemical study of stishovite. *J Solid State Chem* 47:185-200
- Horiuchi H, Hirano M, Ito E, Matsui Y (1982) MgSiO_3 (ilmenite-type): single crystal X-ray diffraction study. *Am Mineral* 67:788-793
- Horiuchi H, Ito E, Weidner DJ (1987) Perovskite-type MgSiO_3 : single-crystal X-ray diffraction study. *Am Mineral* 72:357-360
- Ito E (1977) The absence of oxide mixture in high-pressure phases of Mg-silicates. *Geophys Res Lett* 4:72-74
- Ito E, Matsui Y (1974) High-pressure synthesis of ZnSiO_3 ilmenite. *Phys Earth Planet Int* 9:344-352
- Ito E, Matsui Y (1977) Silicate ilmenites and the post-spinel transformations. *In* *High-Pressure Research Applications in Geophysics*. Manghnani M, Akimoto S (eds) 193-208. New York: Academic Press
- Ito E, Matsui Y (1978) Synthesis and crystal-chemical characterization of MgSiO_3 perovskite. *Earth Planet Sci Lett* 38:443-450
- Ito E, Matsui Y (1979) High-pressure transformations in silicates, germanates, and titanates with ABO_3 stoichiometry. *Phys Chem Minerals* 4:265-273
- Ito E., Weidner DJ (1986) Crystal growth of MgSiO_3 perovskite. *Geophys Res Lett* 13:464-466
- Jackson INS, Liebermann RC, Ringwood AE (1974) Disproportionation of spinels to mixed oxides: significance of cation configuration and implications for the mantle. *Earth Planet Sci Lett* 24:203-208
- Kanzaki M, Stebbins JF, Xue X (1991) Characterization of quenched high pressure phases in CaSiO_3 system by XRD and ^{29}Si NMR. *Geophys Res Lett* 18:463-466

- Kawai N, Tachimori M, Ito E (1974) A high pressure hexagonal form of MgSiO_3 . *Proc Jpn Acad* 50:378
- Kingma KJ, Cohen RE, Hemley RJ, Mao HK (1995) Transformation of stishovite to a denser phase at lower mantle pressures. *Nature* 374:243-245
- Kinomura N, Kume S, Koizumi M (1975) Synthesis of $\text{K}_2\text{SiSi}_3\text{O}_9$ with silicon in 4- and 6-coordination. *Mineral Mag* 40:401-404
- Knoche R, Angel RJ, Seifert F, Fliervoet TF (1998) Complete substitution of Si for Ti in titanite $\text{Ca}(\text{Ti}_{1-x}\text{Si}_x)^{\text{VI}}\text{Si}^{\text{IV}}\text{O}_8$. *Am Mineral* 83:1168-1175
- Kubo A, Suzuki T, Akaogi M (1997) High-pressure phase equilibria in the system CaTiO_3 - CaSiO_3 : stability of perovskite solid solutions. *Phys Chem Minerals* 24:488-494
- Kudoh Y, Ito E, Takeda H (1987) Effect of pressure on the crystal structure of perovskite-type MgSiO_3 . *Phys Chem Minerals* 14:350-354
- Kume S, Matsumoto T, Koizumi M (1966) Dense form of germanate orthoclase (KAlGe_3O_8). *J Geophys Res* 71:4999-5000
- Liebau F (1985) *Structural Chemistry of Silicates*. New York: Springer
- Liebau F, Hesse KF (1971) Die kristallstruktur einer zweiten monoklinen siliciumdiphosphatphase SiP_2O_7 , mit oktaedrisch koordiniertem silicium. *Z Kristallogr* 133:213-224
- Liebermann RC, Jackson I, Ringwood AE (1977) Elasticity and phase equilibria of spinel disproportionation reactions. *Geophys J R Astr Soc* 50:553-586
- Liu LG (1974) Silicate perovskite from phase transformations of pyrope-garnet at high pressure and temperature. *Geophys Res Lett* 1:277-280,
- Liu LG (1975a) Post-oxide phases of forsterite and enstatite. *Geophys Res Lett* 2:417-419
- Liu LG (1975b) Post-oxide phases of olivine and pyroxene and mineralogy of the mantle. *Nature* 258:510-512
- Liu LG (1976a) The post-spinel phase of forsterite. *Nature (London)* 262:770-772
- Liu LG (1976b) The high-pressure phases of MgSiO_3 . *Earth Planet Sci Lett* 31:200-208
- Liu LG (1976c) Orthorhombic perovskite phases observed in olivine, pyroxene and garnet at high pressures and temperatures. *Phys Earth Planet Int* 11:289-298
- Liu LG (1977a) Mineralogy and chemistry of the Earth's mantle above 1000 km. *Geophys J Royal Astron Soc* 48:53-62
- Liu LG (1977b) Post-ilmenite phases of silicates and germanates. *Earth Planet Sci Lett* 35:161-168
- Liu LG (1977c) High pressure NaAlSiO_4 : the first silicate calcium ferrite isotype. *Geophys Res Lett* 4:183-186
- Liu LG (1978a) High-pressure phase transformations of albite, jadeite and nepheline. *Earth Planet Sci Lett* 37:438-444
- Liu LG (1978b) High pressure Ca_2SiO_4 , the silicate K_2NiF_4 -isotype with crystalchemical and geophysical implications. *Phys Chem Minerals* 3:291-299
- Liu LG (1979) On the 650-km seismic discontinuity. *Earth Planet Sci Lett* 42:202-208
- Liu JG (1986) Phase transformations in serpentine at high pressure s and temperatures and implications for subducting lithosphere. *Phys Earth Planet Int* 42:255-262
- Liu JG (1987) Effects of H_2O on the phase behavior of the forsterite-enstatite system at high pressures and temperatures and implications for the earth. *Phys Earth Planet Int* 49:142-167
- Liu LG, Ringwood AE (1975) Synthesis of a perovskite-type polymorph of CaSiO_3 . *Earth Planet Sci Lett* 28:209-211
- Madon M, Castex J, Peyronneau J (1989) A new aluminocalcic high-pressure phase as a possible host of calcium and aluminum in the lower mantle. *Nature* 342:422-425
- Mao HK, Yagi T, Bell PM (1977) Mineralogy of the Earth's deep mantle: quenching experiments on mineral compositions at high pressure and temperature. *Carnegie Inst Wash Yearb* 76:502-504
- Mao HK, Chen LC, Hemley RJ, Jephcoat AP, Wu Y (1989) Stability and equation of state of CaSiO_3 -perovskite to 134 GPa. *J Geophys Res* 94:17889-17894
- Mao, HK, Shen G, Hemley RJ (1997) Multivariant dependence of Fe-Mg partitioning in the lower mantle. *Science* 278:2098-2100
- Marezio M, Remeika JP, Jayaraman A (1966) High-pressure decomposition of synthetic garnets. *J Chem Phys* 45:1821-1824
- Mayer H (1974) Die kristallstruktur von $\text{Si}_5\text{O}[\text{PO}_4]_6$. *Mh Chem* 105:46-54
- McCammon CA (1997) Perovskite as a possible sink for ferric iron in the lower mantle. *Nature* 387:694-696
- McCammon CA (1998) The crystal chemistry of ferric iron in $\text{Fe}_{0.05}\text{Mg}_{0.95}\text{SiO}_3$ perovskite as determined by Mössbauer spectroscopy in the temperature range 80-293 K. *Phys Chem Minerals* 25:292-300
- McHone JF, Nieman RA, Lewis CF, Yates AM (1989) Stishovite at the Cretaceous-Tertiary boundary, Raton, New Mexico. *Science* 243:1182-1184
- Megaw HD (1973) *Crystal Structures: a Working Approach*. Philadelphia: W. B. Saunders

- Modaressi A, Gerardin R, Malaman B, Gleitzer C (1984) Structure et propriétés d'un germanate de fer de valence mixte $\text{Fe}_4\text{Ge}_2\text{O}_9$. Etude succincte de $\text{Ge}_x\text{Fe}_{3-x}\text{O}_4$ ($x \leq 0.5$). *J Solid State Chem* 53:22-34
- Moore PB, Araki T (1974) Pinakiolite, $\text{Mg}_2\text{Mn}^{3+}\text{O}_2[\text{BO}_3]$; warwickite, $\text{Mg}(\text{Mg}_{0.5}\text{Ti}_{0.5})\text{O}[\text{BO}_3]$; wightmanite, $\text{Mg}_5(\text{O})(\text{OH})_5[\text{BO}_3]n\text{H}_2\text{O}$: crystal chemistry of complex 3Å wallpaper structures. *Am Mineral* 59:985-1004
- Nakatsuka A, Yoshiasa A, Yamanaka T, Ohtaka O, Katsura T, Ito E (1999b) Symmetry change of majorite solid-solution in the system $\text{Mg}_3\text{Al}_2\text{Si}_3\text{O}_{12}$ - MgSiO_3 . *Am Mineral* 84:1135-1143
- Nakatsuka A, Yoshiasa A, Yamanaka T, Ito E (1999b) Structure of a birefringent Cr-bearing majorite $\text{Mg}_3(\text{Mg}_{0.34}\text{Si}_{0.34}\text{Al}_{0.18}\text{Cr}_{0.14})_2\text{Si}_3\text{O}_{12}$. *Am Mineral* 84:199-202
- Nevskii NN, Ilyukhin VV, Belov NV (1979a) The crystal structure of CaGe_2O_5 , germanium analog of sphene. *Sov Phys Crystallogr* 24:415-416
- Nevskii NN, Ilyukhin VV, Ivanova LI, Belov NV (1979b) Crystal structure of calcium germanate $\text{Ca}_2\text{Ge}_2[\text{GeO}_4][\text{Ge}_4\text{O}_{12}]$. *Sov Phys Crystallogr* 24:135-136
- Nevskii NN, Ilyukhin VV, Belov NV (1980) Interpretation of the crystal structure of calcium germanate $\text{Ca}_2\text{Ge}_7\text{O}_{16}$ by the symmetrization method. *Sov Phys Crystallogr* 25:89-90
- Nishi F (1996) Strontium tetragermanate SrGe_4O_9 . *Acta Crystallogr C* 52:2393-2395
- Olsen JS, Cousins CSG, Gervard L, Jahns H (1991) A study of the crystal structure of Fe_2O_3 in the pressure range up to 65 GPa using synchrotron radiation. *Phys Scripta* 43:327-330
- Pacalo REG, Gasparik T (1990) Reversals of the orthoenstatite-clinoenstatite transition at high pressures and high temperatures. *J Geophys Res* 95:15853-15858
- Pacalo REG, Parise JB (1992) Crystal structure of superhydrous B, a hydrous magnesium silicate synthesized at 1400°C and 20 GPa. *Am Mineral* 77:681-684
- Pauling L (1960) *The Nature of the Chemical Bond*. (3rd edition) New York: Cornell University Press
- Post JE, Burnham CW (1986) Modeling tunnel-cation displacements in hollandites using structure-energy calculations. *Am Mineral* 71:1178-1185
- Preisinger A (1962) Struktur des stishovits, höchdruck-SiO₂. *Naturwissenschaften* 49:345
- Prewitt CT, Sleight AW (1969) Garnet-like structures of high-pressure cadmium germanate and calcium germanate. *Science* 163:386-387
- Reid AF, Ringwood AE (1969) Six-coordinate silicon: high-pressure strontium and barium aluminosilicate with the hollandite structure. *J Solid State Chem* 1:6-9
- Reid AF, Ringwood AE (1970) The crystal chemistry of dense M_3O_4 polymorphs: high pressure Ca_2GeO_4 of K_2NiF_4 structure type. *J Solid State Chem* 1:557-565
- Reid AF, Ringwood AE (1975) High-pressure modification of ScAlO_3 and some geophysical implications. *J Geophys Res* 80:3363-3369
- Reid AF, Wadsley AD, Ringwood AE (1967) High pressure NaAlGeO_4 , a calcium ferrite isotype and model structure for silicates at depth in the Earth's mantle. *Acta Crystallogr* 23:736-739
- Reid AF, Li C, Ringwood AE (1977) High-pressure silicate pyrochlores, $\text{Sc}_2\text{Si}_2\text{O}_7$ and $\text{In}_2\text{Si}_2\text{O}_7$. *J Solid State Chem* 20:219-226
- Ringwood AE (1962) Mineralogical constitution of the deep mantle. *J Geophys Res* 67:4005-4010
- Ringwood AE (1966) Mineralogy of the mantle. *In Advances in Earth Sciences*. Hurley P (ed) p 357-398. Cambridge, Massachusetts: MIT Press
- Ringwood AE, Major A (1967a) Some high-pressure transformations of geophysical interest. *Earth Planet Sci Lett* 2:106-110
- Ringwood AE, Major A (1967b) High-pressure reconnaissance investigations in the system Mg_2SiO_4 - $\text{MgO-H}_2\text{O}$. *Earth Planet Sci. Lett* 2:130-133
- Ringwood AE, Major A (1971) Synthesis of majorite and other high pressure garnets and perovskites. *Earth Planet Sci Lett* 12:411-418
- Ringwood AE, Reid AF, Wadsley AD (1967) High-pressure KAlSi_3O_8 , an aluminosilicate with six-fold coordination.. *Acta Crystallogr* 23:736-739
- Ringwood AE, Seabrook M (1962) High-pressure transition of MgGeO_3 from pyroxene to corundum structure. *J Geophys Res* 67:1690-1691
- Ross CR, Bernstein LR, Waychunas GA (1988) Crystal structure refinement of stottite, $\text{FeGe}(\text{OH})_6$. *Am Mineral* 73:657-661
- Ross NL, Hazen RM (1990) High-pressure crystal chemistry of MgSiO_3 perovskite. *Phys Chem Minerals* 17:228-237
- Ross NL, Shu J, Hazen RM, Gasparik T (1990) High-pressure crystal chemistry of stishovite. *Am Mineral* 75:739-747
- Sawamoto H (1977) Orthorhombic perovskite (Mg,Fe) SiO_3 and the constitution of the lower mantle. *High-Pressure Research Applications in Geophysics*, Manghnani MH, Akimoto S (eds) p 219-244. New York: Academic Press

- Schmidt MW (1995) Lawsonite: upper pressure stability and formation of higher density hydrous phases. *Am Mineral* 80:1286-1292
- Schmidt MW, Finger LW, Angel RJ, Dinnebrier (1998) Synthesis, crystal structure, and phase relations of AlSiO_3OH , a high-pressure hydrous phase. *Am Mineral* 83:881-888
- Sharp TG, Lingemann CM, Dupas C, Stoffler D (1997) Natural occurrence of MgSiO_3 -ilmenite and evidence for MgSiO_3 -perovskite in a shocked L chondrite. *Science* 277:352-355
- Sinclair W, Ringwood AE (1978) Single crystal analysis of the structure of stishovite. *Nature (London)* 272:714-715
- Smith JV (1982) *Geometrical and Structural Crystallography*. New York: Wiley
- Smith JV, Mason B (1970) Pyroxene-garnet transformation in Coorara meteorite. *Science* 168:832-833
- Smolin YI (1968) Crystal structure of barium tetragermanate. *Dokl Akad Nauk SSSR* 181:595-598
- Smyth JR, Bish DL (1988) *Crystal Structures and Cation Sites of the Rock-Forming Minerals*. Winchester, MA: Allen and Unwin
- Stebbins JF, Kanzaki M (1991) Local structure and chemical shifts for six-coordinated silicon in high-pressure mantle phases. *Science* 251:294-298
- Stishov SM (1995) Memoir on the discovery of high-density silica. *High Pres Res* 13:245-280
- Stishov SM, Belov NV (1962) On the structure of a new dense modification of silica, SiO_2 [in Russian]. *Dokl Akad Nauk SSSR* 143:951-954
- Stishov SM, Popova SV (1961) A new dense modification of silica. *Geokhimiya* 10:837-839
- Subramanian MA, Gopalakrishnan J, Sleight AW (1988) New layered perovskites: AbiNb_2O_7 and $\text{Apb}_2\text{Nb}_3\text{O}_{10}$ (A = Rb or Cs). *Mater Res Bull* 23:837-842
- Sugiyama M., Endo E, Koto K (1987) The crystal structure of stishovite under pressure to 6 GPa. *Mineral J (Japan)* 13:455-466
- Swanson DK, Prewitt CT (1983) The crystal structure of $\text{K}_2\text{Si}^{\text{VI}}\text{Si}_3^{\text{IV}}\text{O}_9$. *Am Mineral* 68:581-585
- Thompson JB Jr (1978) Biopyriboles and polysomatic series. *Am Mineral* 63:239-249
- Tillmanns E, Gebert W, Baur WH (1973) Computer simulation of crystal structures applied to the solution of the superstructure of cubic silicodiphosphate. *J Solid State Chem* 7:69-84
- Tomioka N, Fujino K (1997) Natural (Mg,Fe) SiO_3 -ilmenite and -perovskite in the Tenham meteorite. *Science* 277:1084-1086
- Tsuchida Y and Yagi T (1989) A new, post-stishovite high-pressure polymorph of silica. *Nature* 340:217-220
- Vicat J, Fanchon E, Strobel P, Qui DT (1986) The structure of $\text{K}_{1.33}\text{Mn}_8\text{O}_{16}$ and cation ordering in hollandite-type structures. *Acta Crystallogr B* 42:162-167
- Voellenkle H, Wittmann H, Nowotny H (1969) Die Kristallstruktur der Verbindung $\text{LiNa}[\text{Ge}_4\text{O}_9]$. *Mh Chem* 100:79-90
- Voellenkle H, Wittmann H (1971) Die Kristallstruktur des Kaliumtetragermanats $\text{K}_2[\text{Ge}_4\text{O}_9]$. *Mh Chem* 102:1245-1254
- Von Dreele RB, Bless PW, Kostiner E, Hughes RE (1970) The crystal structure of magnesium germanate: a reformulation of Mg_4GeO_6 as $\text{Mg}_{28}\text{Ge}_{10}\text{O}_{48}$. *J Solid State Chem* 2:612-618
- Wadsley AD (1964) Inorganic non-stoichiometric compounds. In *Non-Stoichiometric Compounds*. Mandelcoin L (ed) p 111-209. New York: Academic Press
- Yagi A, Suzuki T, Akaogi M (1994) High pressure transitions in the system KAlSi_3O_8 - $\text{NaAlSi}_3\text{O}_8$. *Phys Chem Minerals* 21:12-17
- Yagi T, Mao HK, Bell PM (1978) Structure and crystal chemistry of perovskite-type MgSiO_3 . *Phys Chem Minerals* 3:97-110
- Yagi T, Mao HK, Bell PM (1982) Hydrostatic compression of perovskite-type MgSiO_3 . In *Advances in Physical Geochemistry*. Saxena SK (ed) 317-325. Berlin: Springer
- Yamada H., Matsui Y, Ito E (1983) Crystal-chemical characterization of NaAlSiO_4 with the CaFe_2O_4 structure. *Mineral Mag* 47:177-181
- Yamada H, Matsui Y, Ito E. (1984) Crystal-chemical characterization of KAlSi_3O_8 with the hollandite structure. *Mineral J (Japan)* 12:29-34
- Yang H, Prewitt CT, Frost DJ (1997) Crystal structure of the dense hydrous magnesium silicate, phase D. *Am Mineral* 82:651-654
- Zhang J, Ko J, Hazen RM, Prewitt CT (1993) High-pressure crystal chemistry of KAlSi_3O_8 hollandite. *Am Mineral* 78:493-499